New Results from Jefferson Lab on Exclusive, Forward π^-/π^+ Electroproduction from Deuterium

Garth Huber

UNIVERSITY OF REGINA

MAMI A2 Collaboration, December 9, 2014.

Confinement in QCD

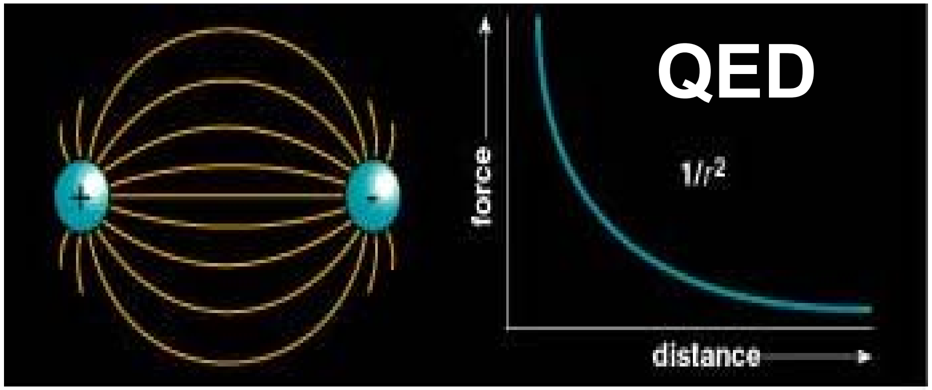

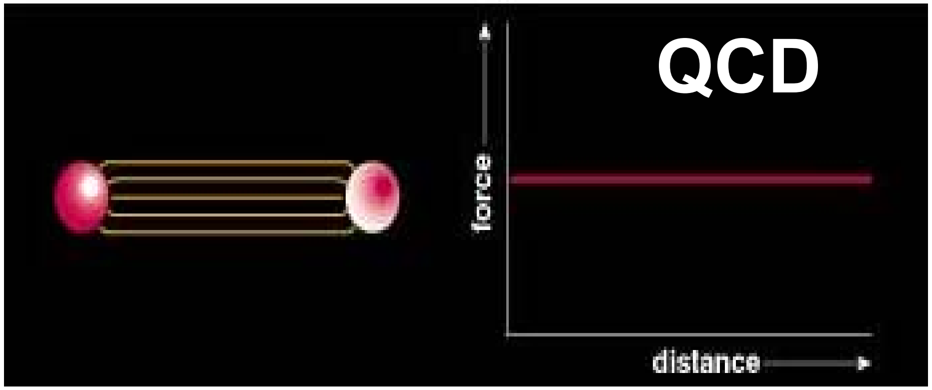

- Unlike the photons of QED, the gluons of QCD carry color charge and interact strongly, leading to the confinement of quarks inside hadrons.
- The quantitative understanding of confinement is still an open challenge for physics!

QCD's Dual Nature

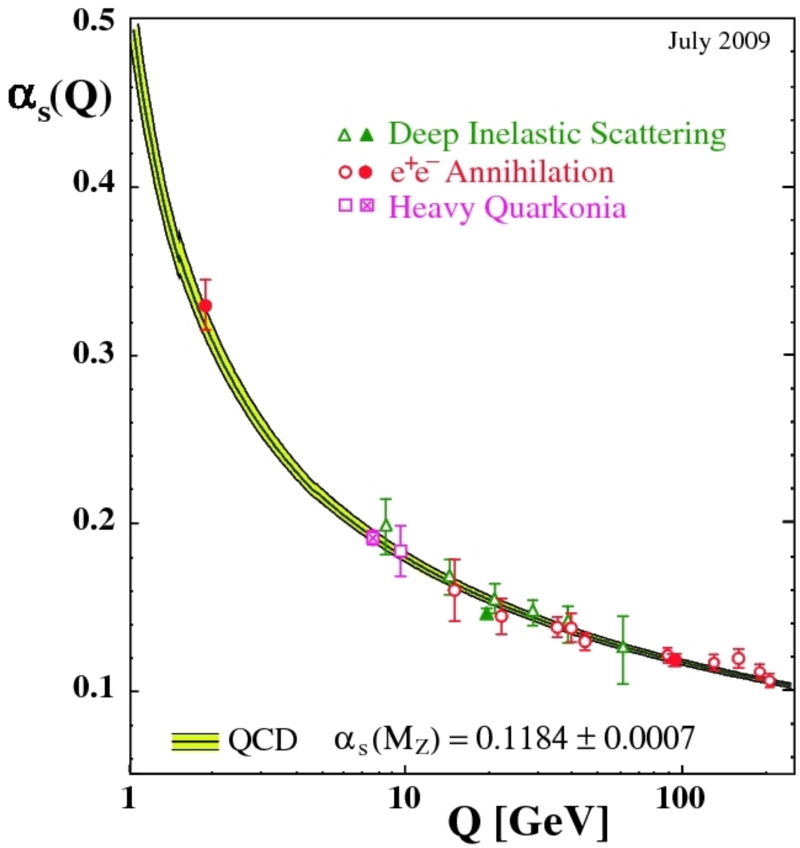

Short Distance Interaction:

- Short distance quark-quark interaction is feeble.
  - Quarks inside protons behave as if they are nearly unbound.
  - Asymptotic Freedom.
- perturbative QCD (pQCD).

Long Distance Interaction:

- Quarks strongly bound within hadrons.
  - Color confinement (strong QCD).
- QCD calculations extremely difficult.
- **QCD-based models often used, but experimental data needed to validate approaches used.**
- **Studies are at the interface of particle and nuclear physics since the problems often require a "many body" approach.**

Soft-Hard Factorization in QCD

- **A basic assumption of the quark-parton model.**
- In QCD, it can be shown that the DIS cross section may be written as a convolution of:
  1. Perturbatively-calculable hard scattering cross-section
  2. Non-perturbative parton density.

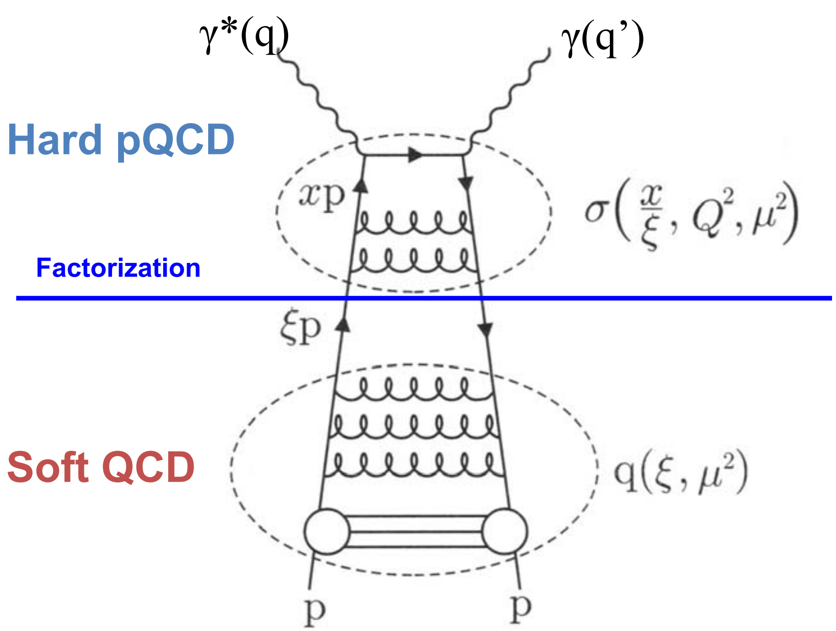

e.g. Virtual Compton scattering

Hard gluon radiative corrections included in γ^*q scattering cross section

Ladder of soft gluon radiative corrections included in probability to find quark in proton with momentum fraction ξ

- **Factorization does not apply everywhere!**
- The *Factorization Regime* is the hard-scattering kinematics where gluon ladder division applies.

Deep Exclusive Scattering

- In Deep Exclusive Scattering, all final state particles are either detected or inferred via missing mass.
- Experiments are demanding, since exclusive cross sections are small, and multiple particles must be detected in coincidence with sufficient resolution to ensure exclusivity.

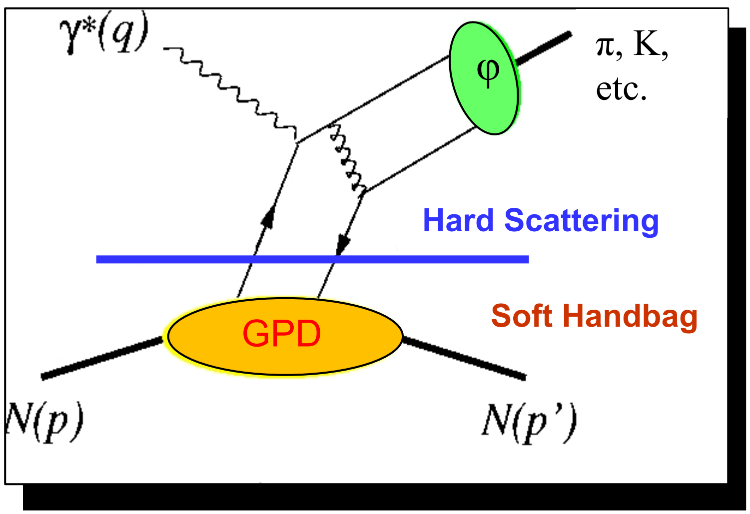

Deep Exclusive Scattering allows some simplifications at sufficiently high Q^2, where the Soft-Hard factorization theorem applies.

[Collins, Frankfurt, Strikman, 1997]

Deep Exclusive $\pi^{\pm}$ Production

- **Single π^+ produced from proton, or π^- from neutron at high momentum transfer.**
- **Can form ratios of separated cross-sections for which non-perturbative corrections may partially cancel, yielding insight into Soft-Hard factorization at modest Q^2.**

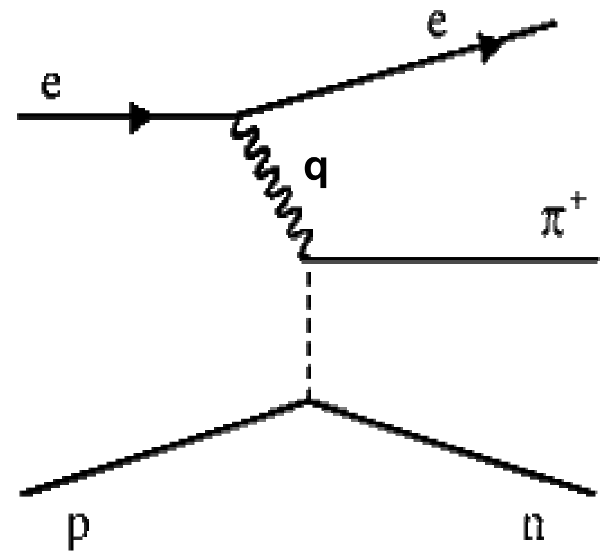

$$R_T = \frac{\gamma_T^* n \to \pi^- p}{\gamma_T^* p \to \pi^+ n} \xrightarrow[high\ -t]{} \frac{2Q_d^2}{2Q_u^2} = \frac{(-1/3)^2}{(+2/3)^2} = \frac{1}{4}$$

A. Nachtmann, Nucl. Phys. **B 115** (1976) 61.

- **Pseudoscalar meson production has been identified as especially sensitive to chiral-odd transverse GPDs.**

  → R_T is not complicated by the π–pole term.

At low $-t$, Meson-Nucleon Degrees of Freedom

- $\pi^{\pm}$ *t*-channel diagram is purely isovector (G-parity conservation).

$$R_L = \frac{\sigma_L[n(e,e'\pi^-)p]}{\sigma_L[p(e,e'\pi^+)n]} = \frac{|A_V - A_S|^2}{|A_V + A_S|^2}$$

- A significant deviation of R_L from unity would indicate the presence of isoscalar backgrounds (such as b_1(1235) contributions to *t*-channel).

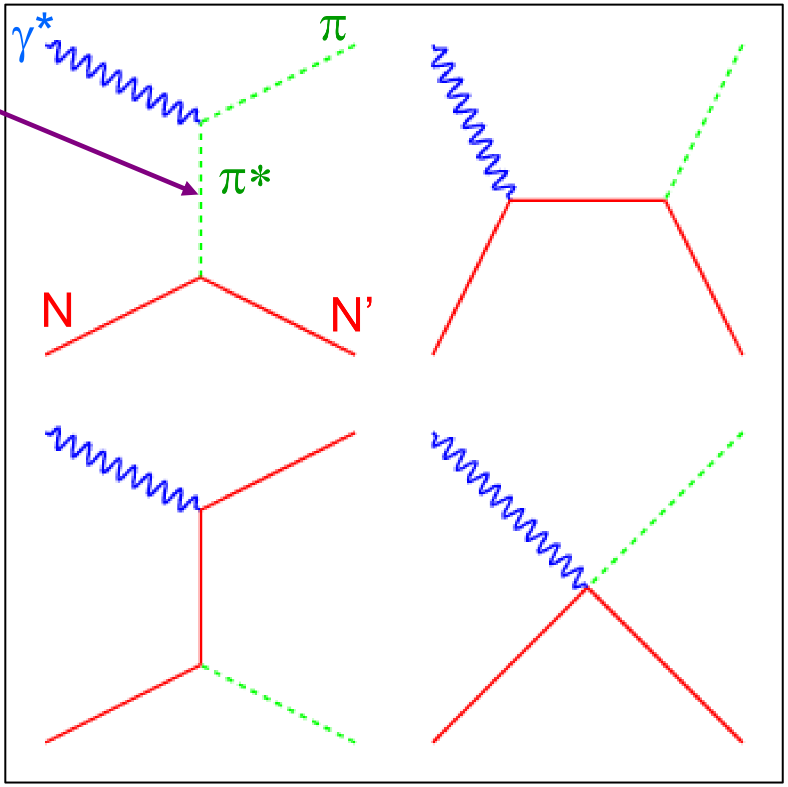

Relevant for extraction of pion form factor from $p(e,e'\pi^+)n$ data, which uses a model including some isoscalar background.

Only Prior ^{2}H(e,e'$\pi^{\pm}$)NN Data

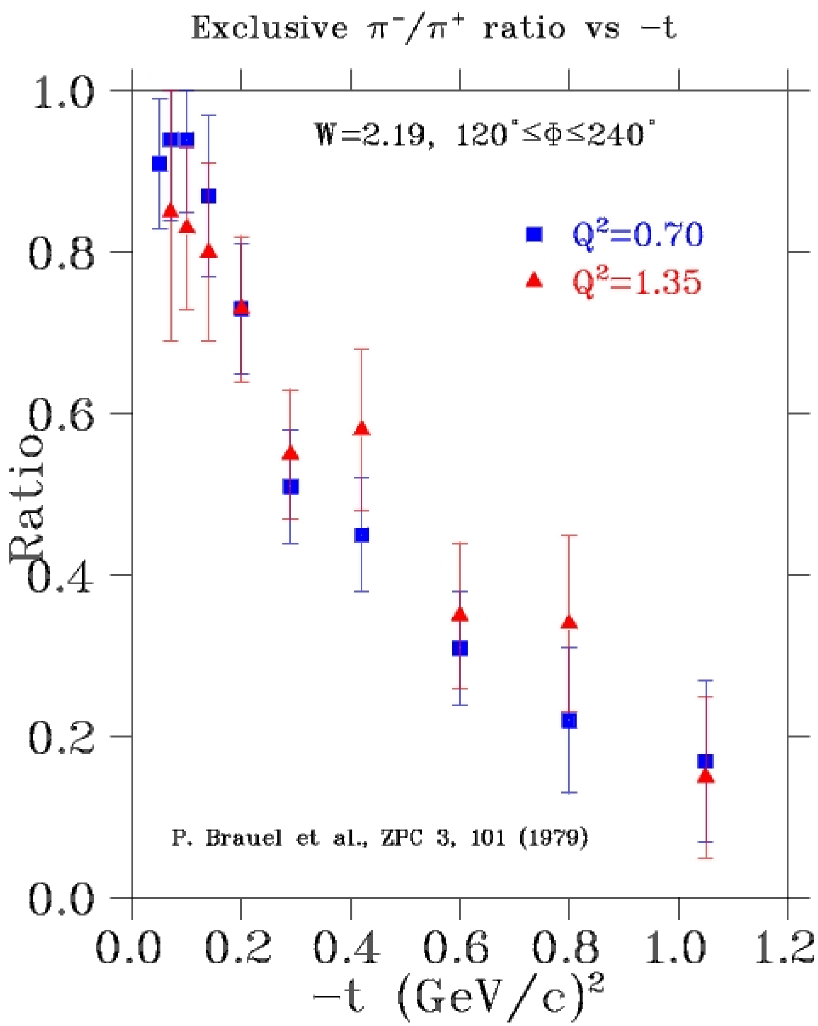

- Only prior exclusive ^{2}H(e,e'$\pi^{\pm}$)NN data was obtained at DESY in the 1970's.
  - Unseparated cross sections only, due to incomplete azimuthal coverage.
  - Q^2=0.70, 1.35 GeV^2.
- **π^-/π^+ ratio intriguingly approaches Nachtmann's quark counting ratio $\rightarrow$1/4 at high $-t$.**
- **Ratio approaches π pole dominance $\rightarrow$1 at low $-t$.**
- Need separated ^{2}H(e,e'$\pi^{\pm}$)NN data over a wide kinematic range to better interpret ratios!

‘Simple’ Longitudinal-Transverse Separation

- Determine $\sigma_T + \varepsilon\, \sigma_L$ for high and low ε in each t-bin for each Q^2
- Isolate σ_L, by varying virtual photon polarization, ε
- Requires uniform detector acceptance

$$\varepsilon = [1+2(1+\tau)\tan^2(\theta/2)]^{-1}$$

$$2\pi \frac{d\sigma}{dt\,d\phi} = \varepsilon \frac{d\sigma_L}{dt} + \frac{d\sigma_T}{dt}$$

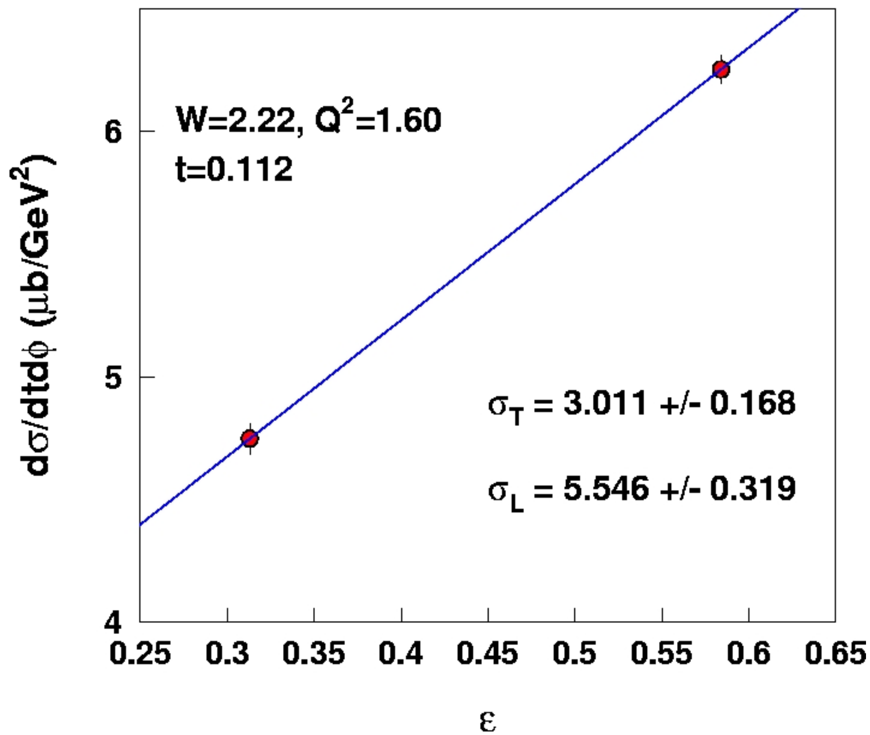

‘More Realistic’ L-T-LT-TT Separation

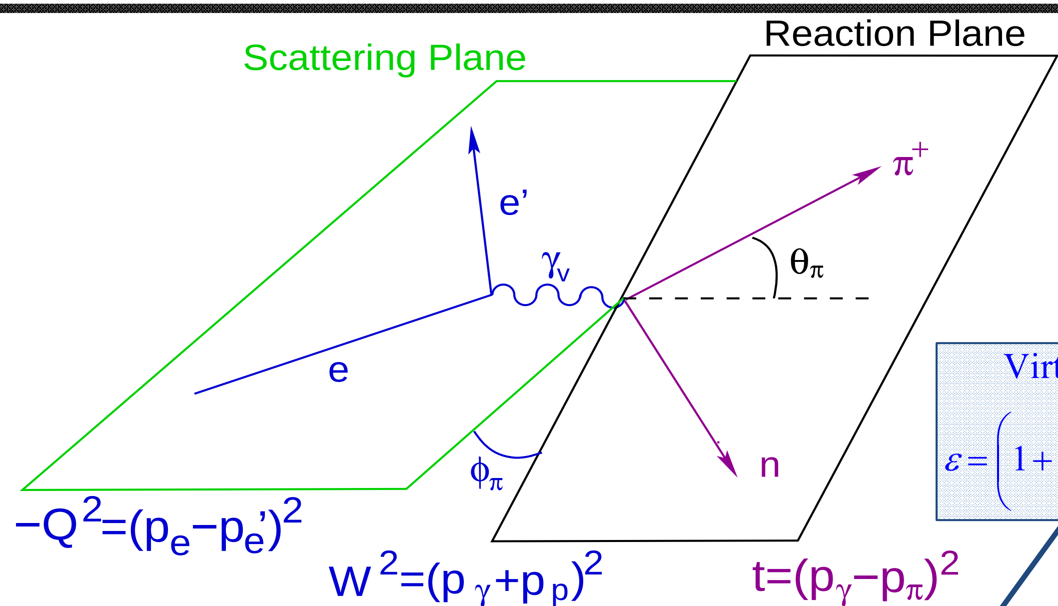

Virtual-photon polarization:

$$\varepsilon = \left(1 + 2\frac{(E_e - E_{e'})^2 + Q^2}{Q^2}\tan^2\frac{\theta_{e'}}{2}\right)^{-1}$$

$$2\pi\frac{d\sigma}{dt\,d\phi} = \varepsilon\frac{d\sigma_L}{dt} + \frac{d\sigma_T}{dt} + \sqrt{2\varepsilon(\varepsilon+1)}\frac{d\sigma_{LT}}{dt}\cos\phi + \varepsilon\frac{d\sigma_{TT}}{dt}\cos 2\phi$$

1. At small $-t$, σ_L has maximum contribution from the π pole.
2. Need to investigate t dependence at relatively fixed Q^2, W, but only three of Q^2, W, t, θ_π are independent.
   - Vary θ_π to measure t dependence.
   - Since non-parallel data needed, LT and TT must also be determined.

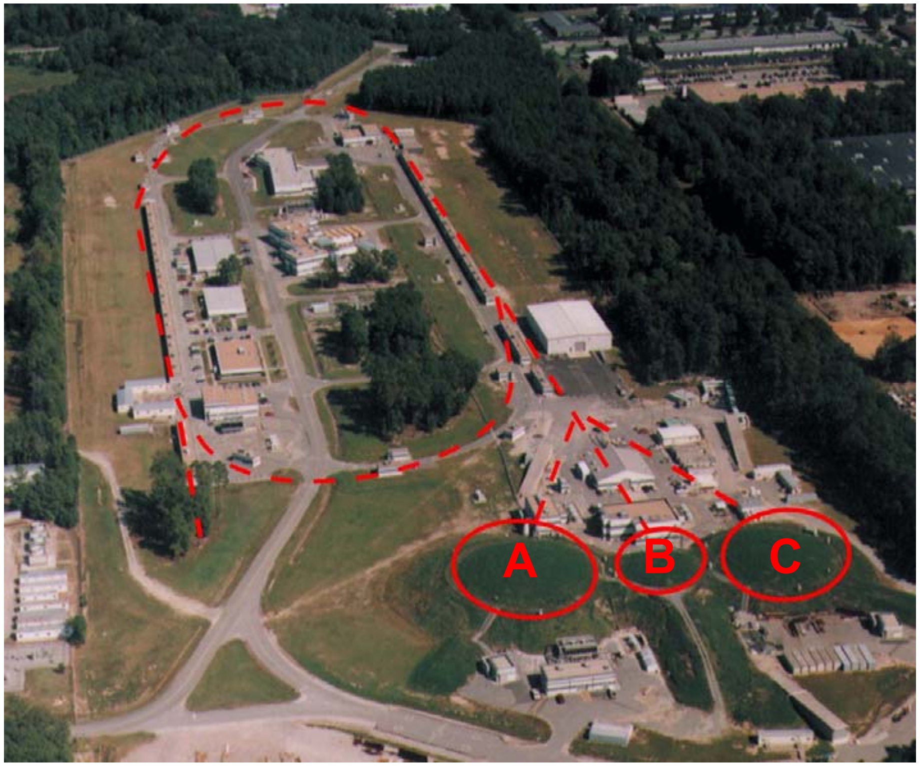

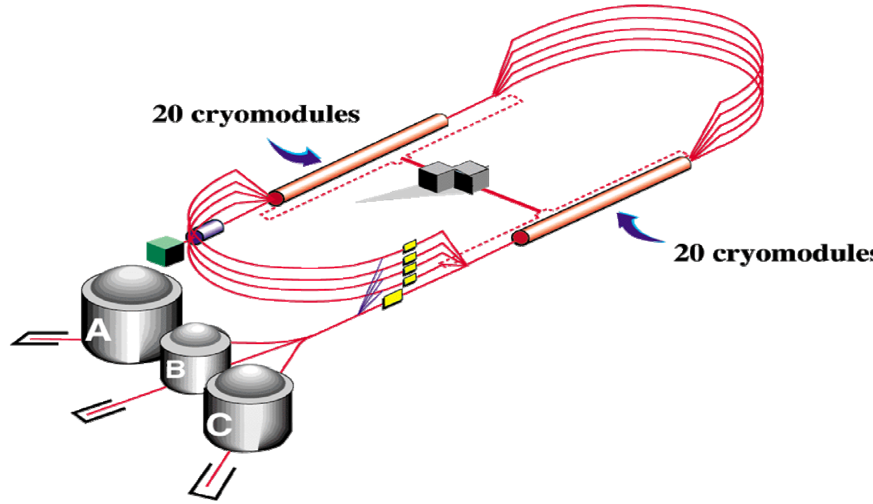

6 GeV Era: 1994-2012

Two Cold Superconducting Linacs
Continuous Polarized Electron Beam

$E \rightarrow 6$ GeV
$> 100\ \mu A$
up to 80% polarization
concurrent to 3 Halls

Jefferson Lab 6 GeV Era - Hall C Setup

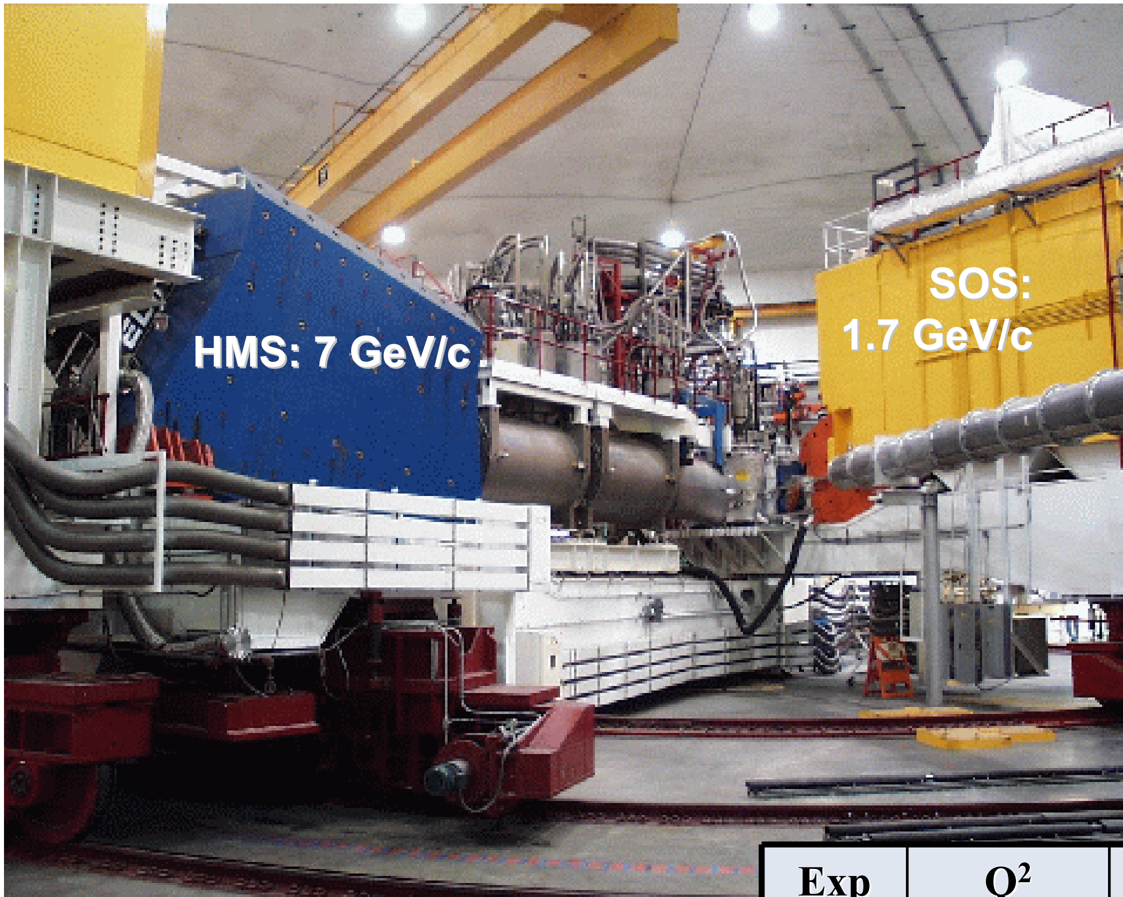

Hall C spectrometers:

- Coincidence measurement.
- SOS detects e^-.
- HMS detects π^+ and π^-.

Targets:

- Liquid 4-cm H/D cells.
- Al target for empty cell measurement.
- ^{12}C solid targets for optics calibration.

Exp	Q^2 $(GeV/c)^2$	W (GeV)	$\lvert t_{min} \rvert$ $(Gev/c)^2$	E_e (GeV)
Fπ-1	0.6-1.6	1.95	0.03-0.150	2.445-4.045
Fπ-2	2.45	2.22	0.189	4.210-5.246

F_π-2 Experimental Setup

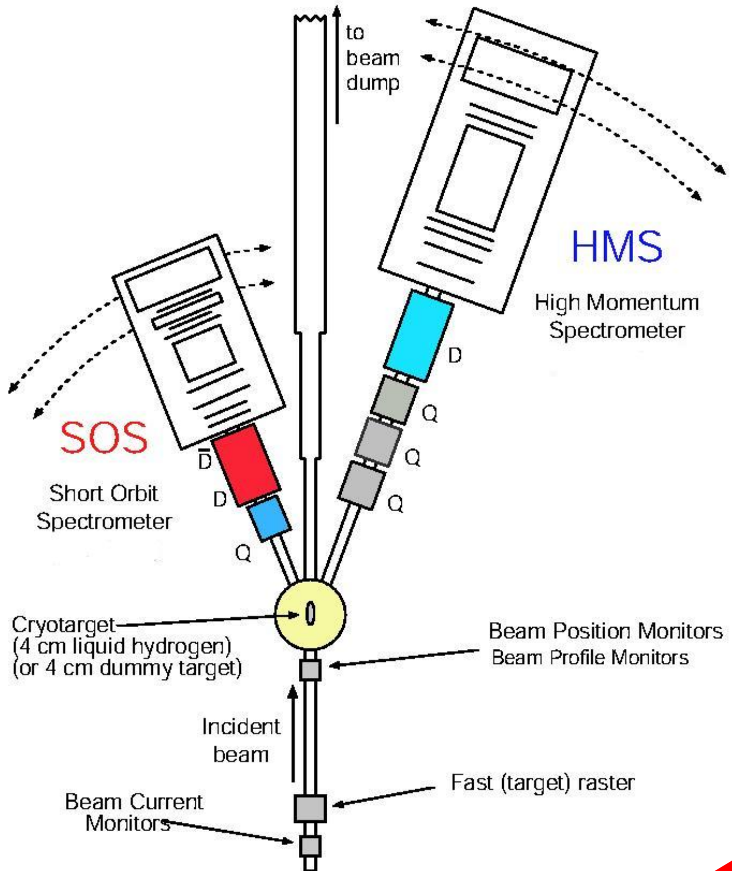

Hall C spectrometers:

- Coincidence measurement.
- SOS detects e^-.
- HMS detects π^+ or π^-.

Targets:

- Liquid 4-cm H/D cells.
- Al (dummy) target for background measurement.
- ^{12}C solid targets for optics calibration.

HMS Aerogel:

- First use in 2003.
- Built by Yerevan group [Nucl. Instrum. Meth. **A548**(2005)364]

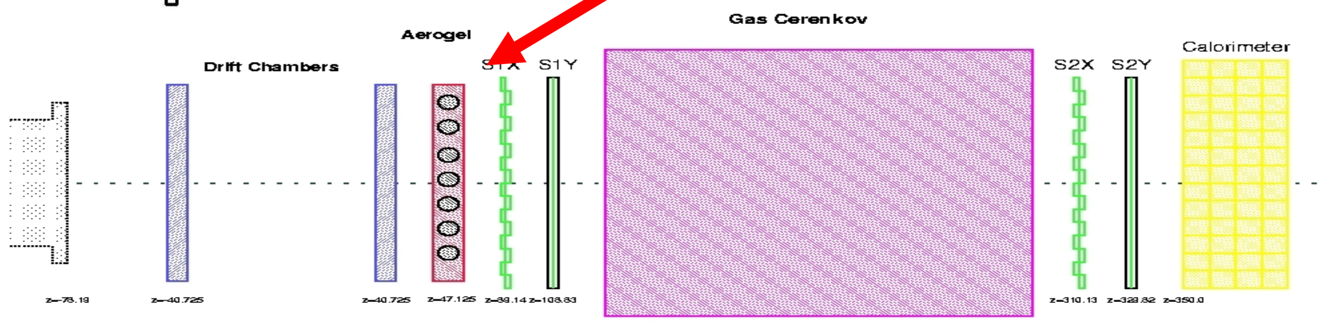

$^{2}H(e,e'\pi^{\pm})NN$ Event selection

Pions detected in HMS – Cerenkov & Coincidence time for PID

Electrons detected in SOS –Cerenkov & Lead Glass Calorimeter

Coincidence time resolution ~200-230 ps.

Cut value ±1 ns.

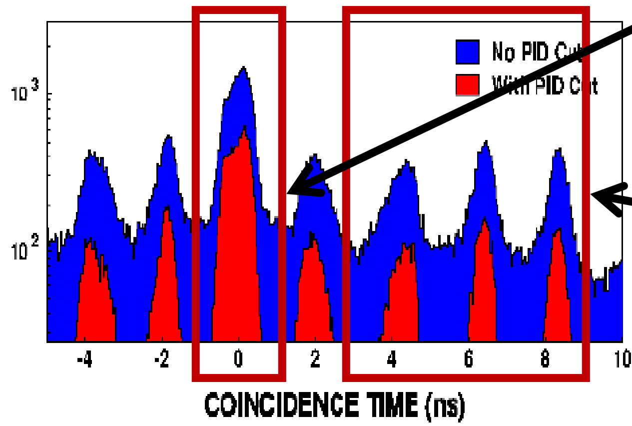

Electron-pion coincidences

Random coincidences

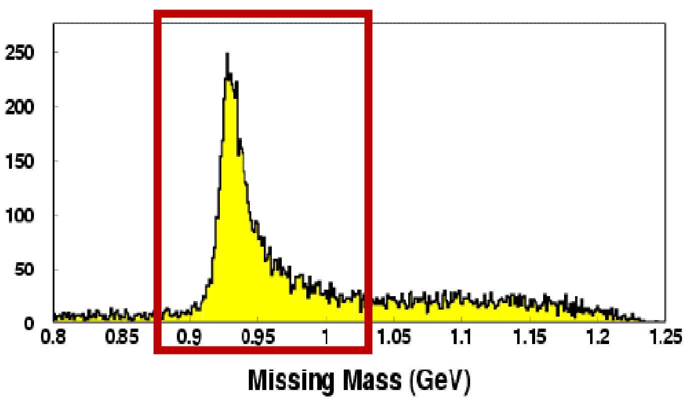

Exclusivity assured via $0.875<MM<1.03$ GeV cut

After PID & MM cuts, almost no random coincidences remain.

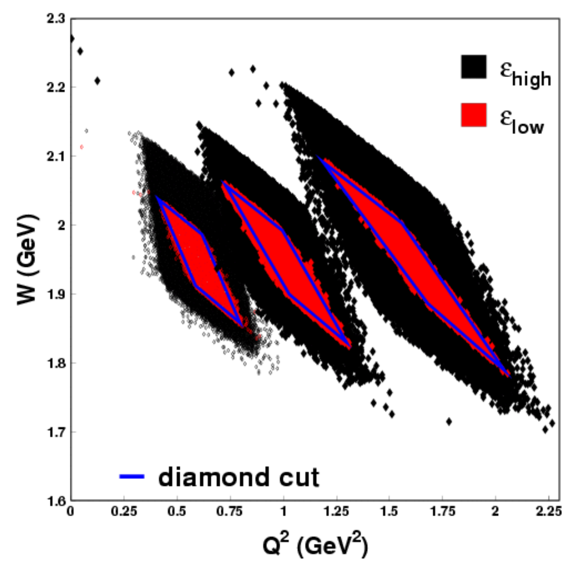

Diamond cuts define common (W,Q^2) coverage at both ε.

Corrections to π^-, π^+ Data

- **Negative polarity of HMS field for $^2H(e,e'\pi^-)pp$ means these runs have high electron rates not shared by $^2H(e,e'\pi^+)nn$ runs.**
- **Understanding rate dependent corrections very important with respect to separated π^-/π^+ ratios.**
  - Improved high rate HMS tracking algorithm.
  - More accurate high rate tracking efficiencies (91-98%).
  - HMS π^- misidentification correction due to e^- pileup in Čerenkov (13%/MHz e^-).
  - High current ^{2}H target boiling correction (4.7%/100μA) for old `beer can' target cell and square beam raster.

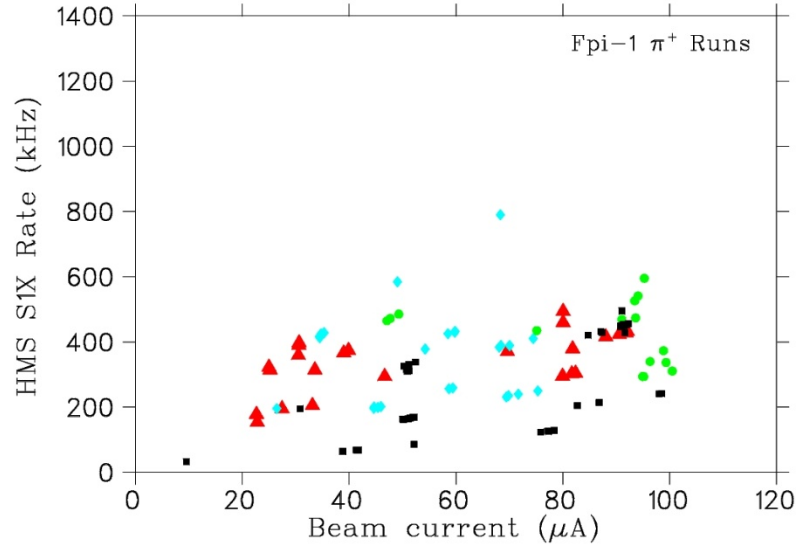

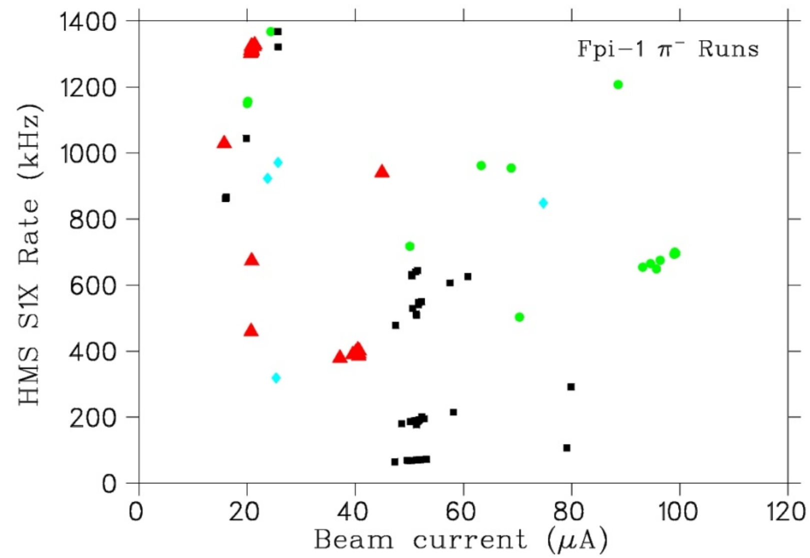

Q^2=0.60, 0.75, 1.0, 1.6 GeV^2

Carbon Luminosity Scans

- To better understand HMS tracking efficiencies, the normalized yields from carbon target were studied vs. rate and vs. current.
  - Carbon target should not “boil”, so normalized yields should be flat vs. current if all efficiencies are calculated correctly.
- Unfortunately, no ^{12}C luminosity scans were taken at different beam currents in the F_π-1 experiment.
  → Conclusions from the F_π-2 study will have to be applied.

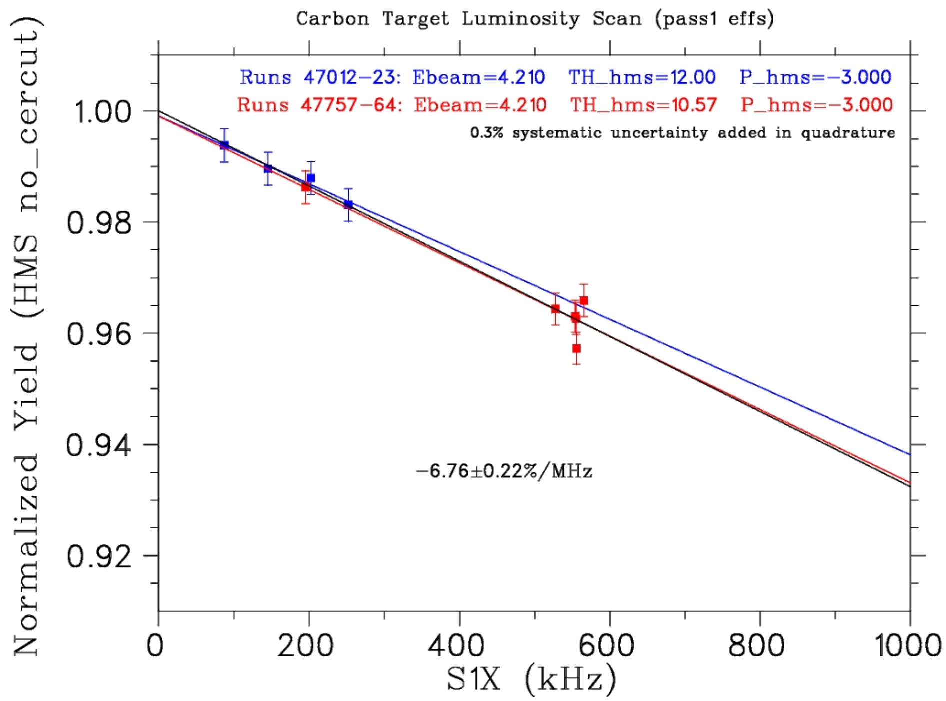

Carbon Scans After Tracking Correction Applied

$$htr\_corrected = htr\_old \times (1 - S1Xrate(kHz) * 6.76236 \times 10^{-5})$$

- Correction is applied to both F_π-1 and F_π-2 tracking efficiencies.
- Particularly important for F_π-1 $^2H(e,e'\pi^-)$ data, with HMS rate up to 1.4 MHz.

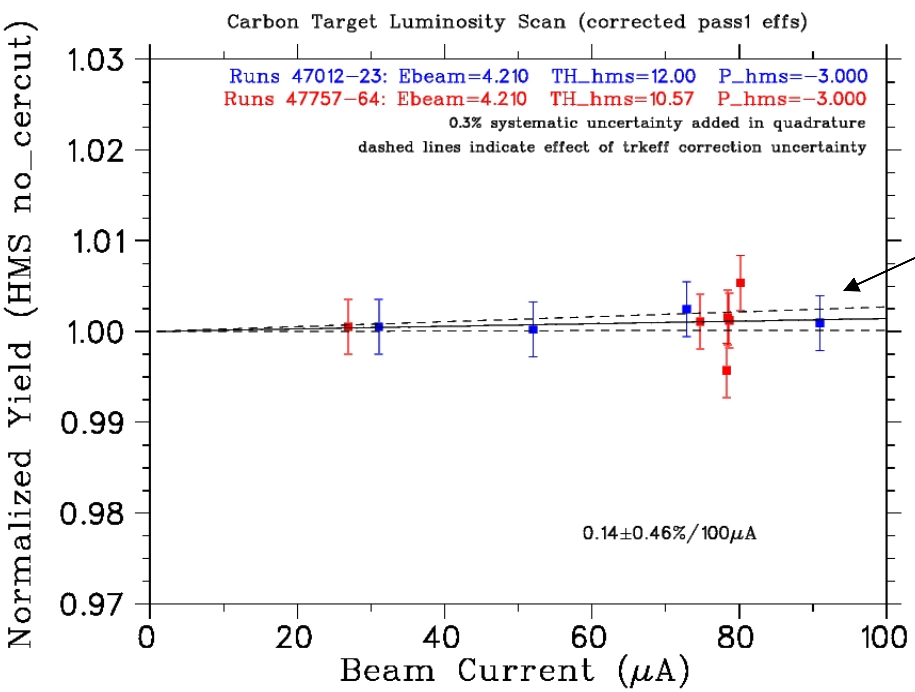

After application of correction, carbon normalized yields show NO residual current dependence.

^{2}H Cryotarget Boiling Corrections

- **After the tracking efficiencies are finalized, the cryotarget boiling corrections can be determined.**

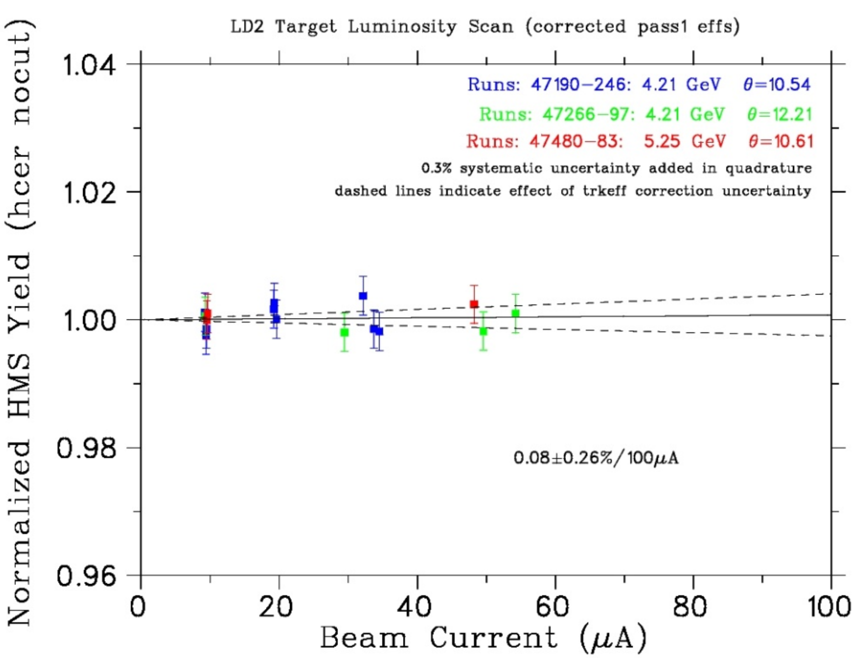

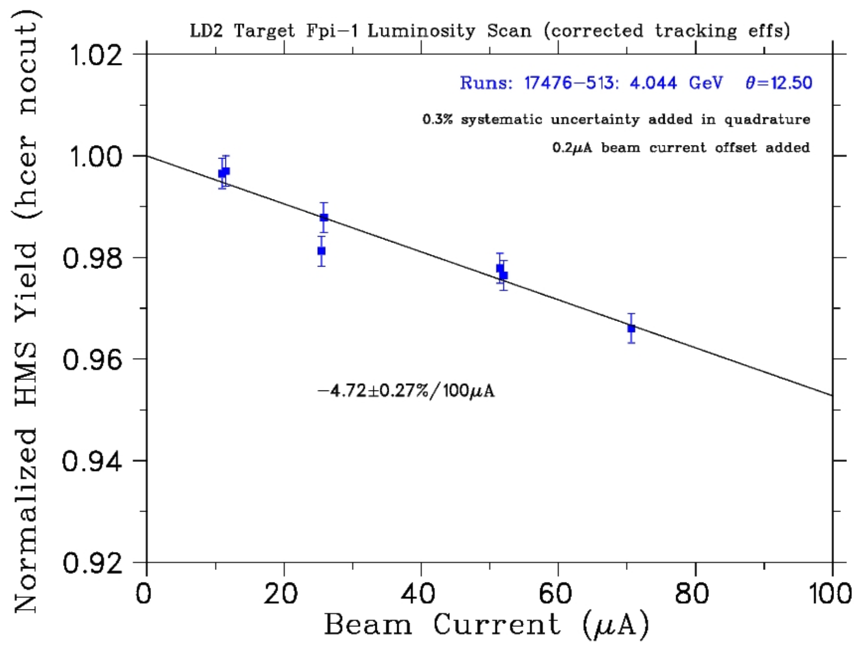

F_π-2: “tuna can” target cell and uniform circular rastering.

- Consistent with no ^{1}H cell correction in T. Horn F_π-2 analysis.

F_π-1: “beer can” target cell and non-uniform square rastering.

- Consistent with 6±1% ^{1}H cell correction in J. Volmer F_π-1 analysis.

HMS Čerenkov Blocking Correction (π^-)

- **In both F_π-1,2, the HMS gas Čerenkov was used as a veto in the trigger for $^2H(e,e'\pi^-)$ runs**
  - **→ needed to avoid high DAQ deadtime due to large e^- rates in HMS.**
- **Čerenkov Blocking:**

  π^- are lost when e^- pass through the gas Čerenkov within ~100ns after π^- has traversed the detector.
  → results in mis-identification of π^- as e^-
- Actual veto thresholds vary according to PMT gain variations at high rates.
  - slightly more restrictive software thresholds are applied in the analysis:
  - F_π-1: accept < 1.5 hcer_npe
  - F_π-2: accept < 2 hcer_npe

HMS Čerenkov Blocking Correction (π^-)

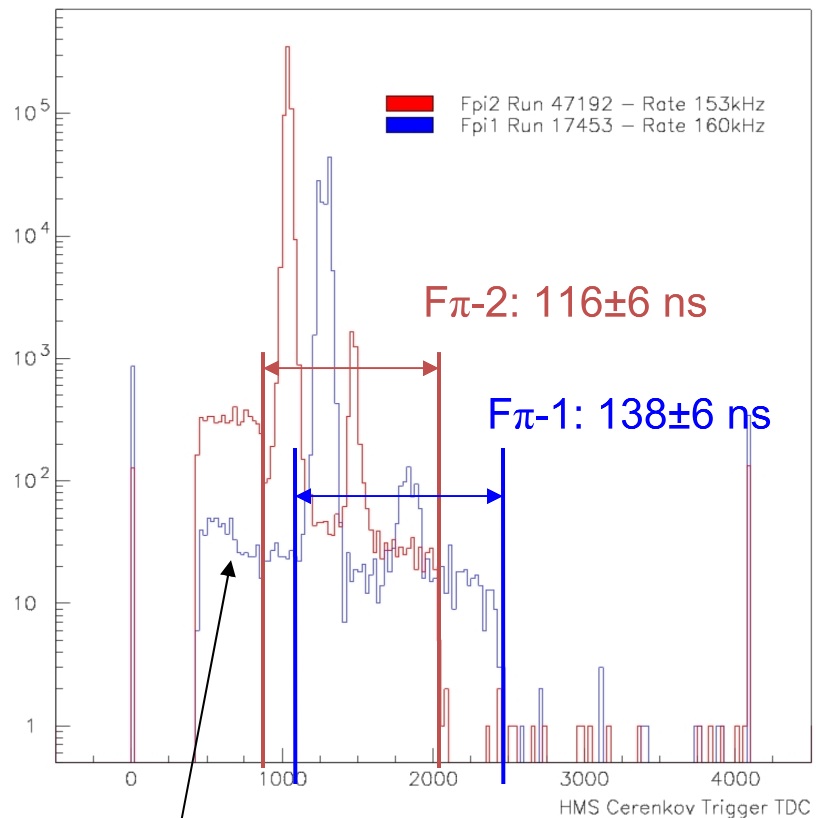

- Region due to early e- passing through detector before e- associated with trigger.
- Already addressed in coincidence time blocking correction.

- Čerenkov Blocking Correction is obtained from Trigger TDC information, since that is independent of tracking efficiency and cryotarget corrections.
- Result is consistent with τ from other studies (not shown here) within statistical errors.

$$\delta_{CCblock} = e^{-ELLOrate \cdot \tau}$$

F_π-2: τ = 115±6 ns

F_π-1: τ = 138±6 ns

Extract Response Functions through Iterative Procedure

Improve φ coverage by taking data at multiple π (HMS) angles, $-4^o<\theta_{\pi q}<4^o$.

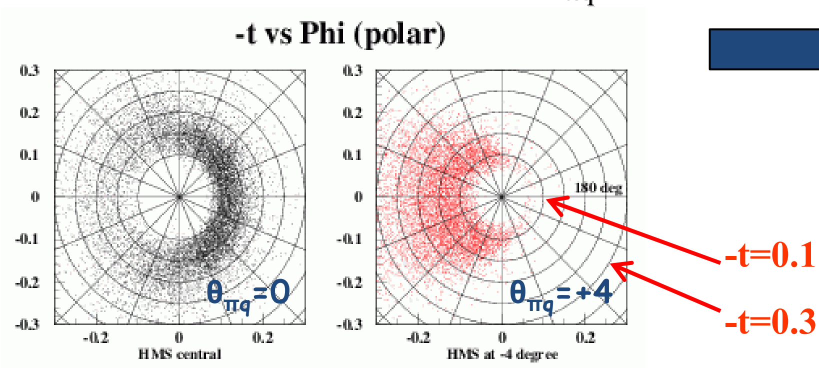

For each π HMS setting, form ratio:

$$R=\frac{Y_{EXP}}{Y_{SIMC}}$$

Combine ratios for π settings together, propagating errors accordingly.

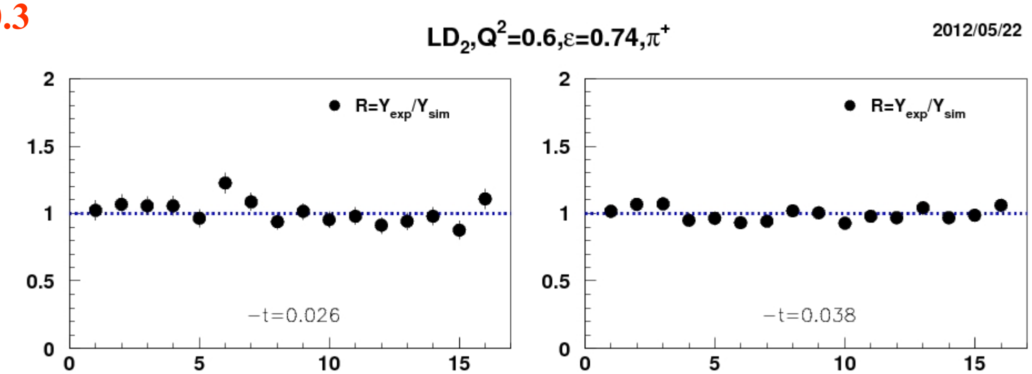

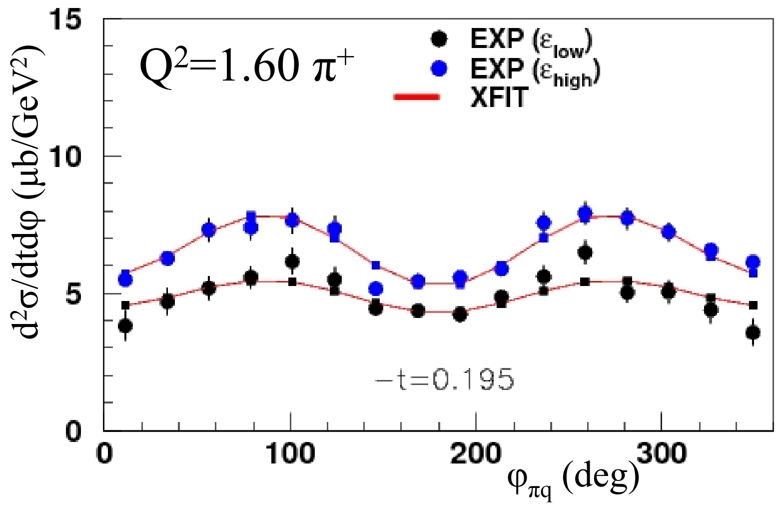

Extract via simultaneous fit of L,T,LT,TT

$$\frac{d^2\sigma}{dtd\varphi}_{EXP}=\left(\frac{Y_{EXP}}{Y_{SIMC}}\right)\frac{d^2\sigma}{dtd\varphi}_{SIMC}$$

$$2\pi\frac{d\sigma}{dtd\phi}=\varepsilon\frac{d\sigma_L}{dt}+\frac{d\sigma_T}{dt}+\sqrt{2\varepsilon(\varepsilon+1)}\frac{d\sigma_{LT}}{dt}\cos\phi+\varepsilon\frac{d\sigma_{TT}}{dt}\cos 2\phi$$

$^2H(e,e'\pi^{\pm})NN$ Separated dσ/dt

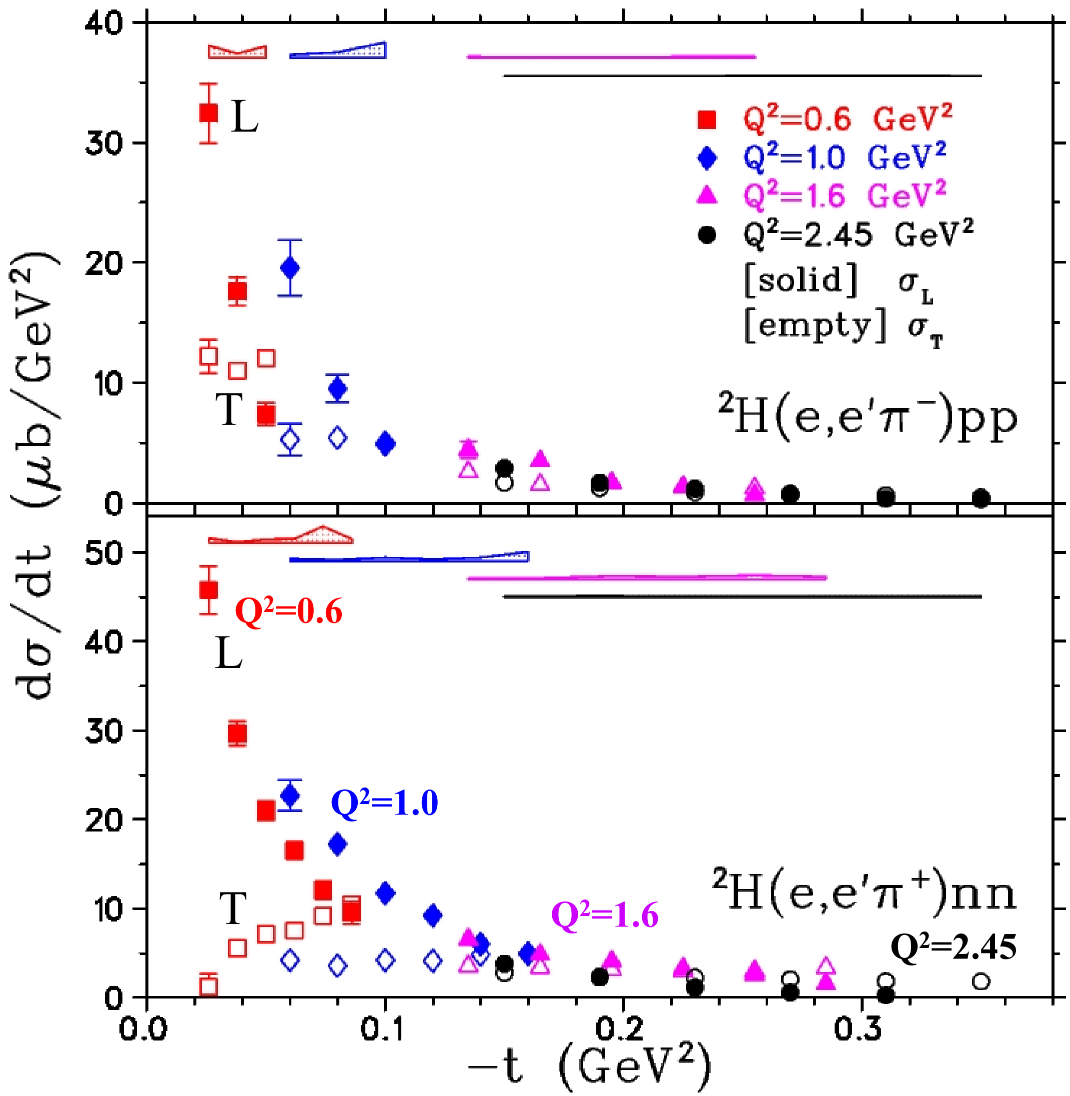

- Data points have slightly different $\overline{W}, \overline{Q}^2$
- All data scaled to W=2.0 GeV assuming $1/(W^2-M^2)$ dependence, M=free nucleon mass.
- No scaling applied in Q^2.

- **Longitudinal cross-section shows steep rise due to π pole at small –t.**
- **Transverse cross-section much flatter.**
- **Both follow nearly universal curves vs –t, with weak Q^2-dependence.**

Error bars indicate statistical and pt-pt systematic uncertainties in quadrature.
Bands indicate L,LT,TT MC model dependence systematic uncertainty.

π^-/π^+ Separated Response Function Ratios

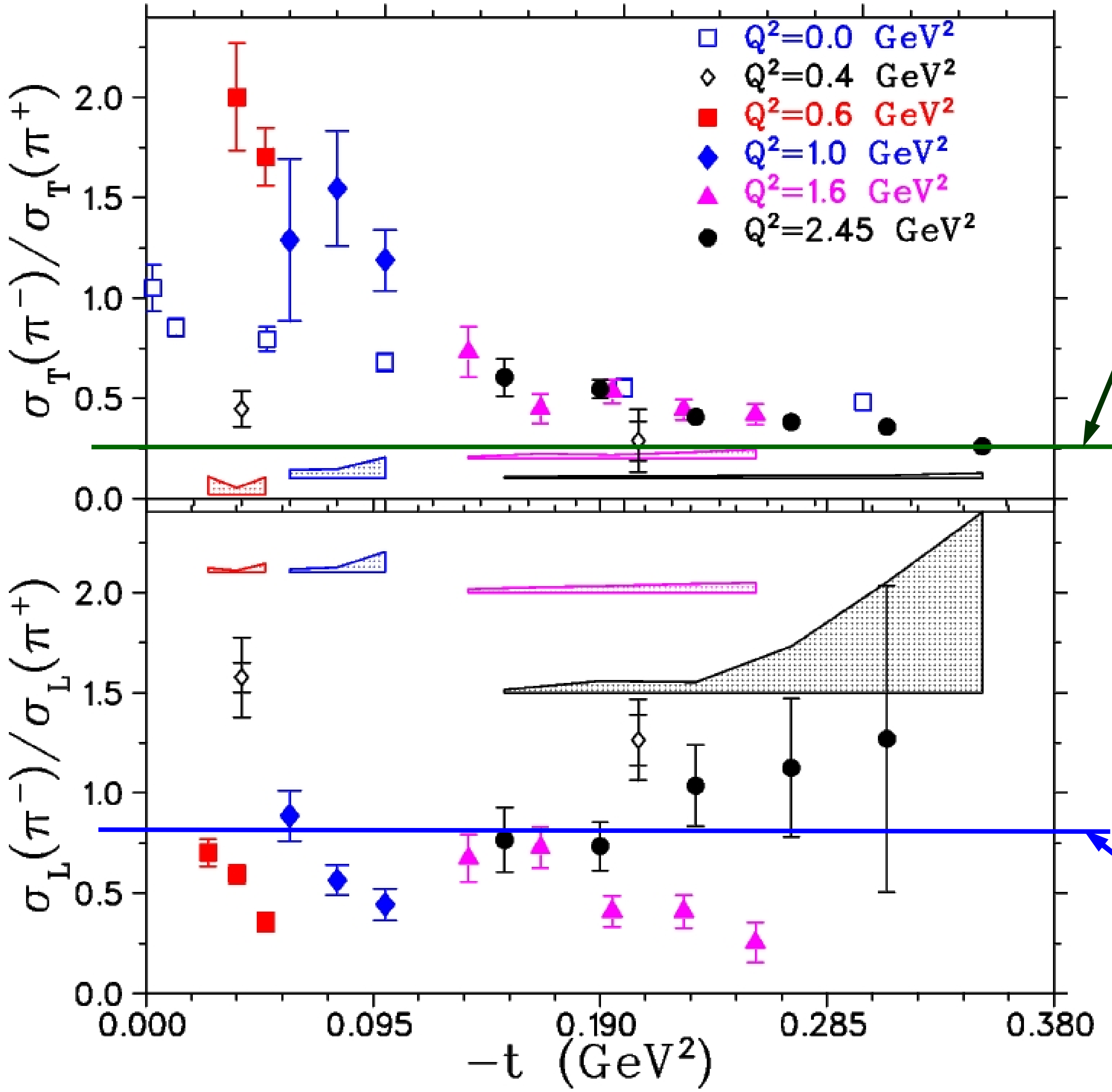

- **Transverse Ratios tend to ¼ as –t increases:**

  → Is this an indication of Nachtmann's quark charge scaling?

- **-t=0.3 GeV^2 seems too low for this to apply. Might indicate the partial cancellation of soft QCD corrections in the formation of the ratio.**

***R_L*≈0.8 near –*t_{min}* at each *Q^2*.**
Predicted in large *N_c* limit calculation.
Frankfurt, et al.
PRL **84**(2000)2589.

Error bars indicate statistical and pt-pt systematic uncertainties in quadrature.
Bands indicate MC model dependence systematic uncertainty.

Dr. Garth Huber, Dept. of Physics, Univ. of Regina, Regina, SK S4S0A2, Canada.

σ_L/σ_T and σ_{TT}/σ_T Ratios for π^+, π^-

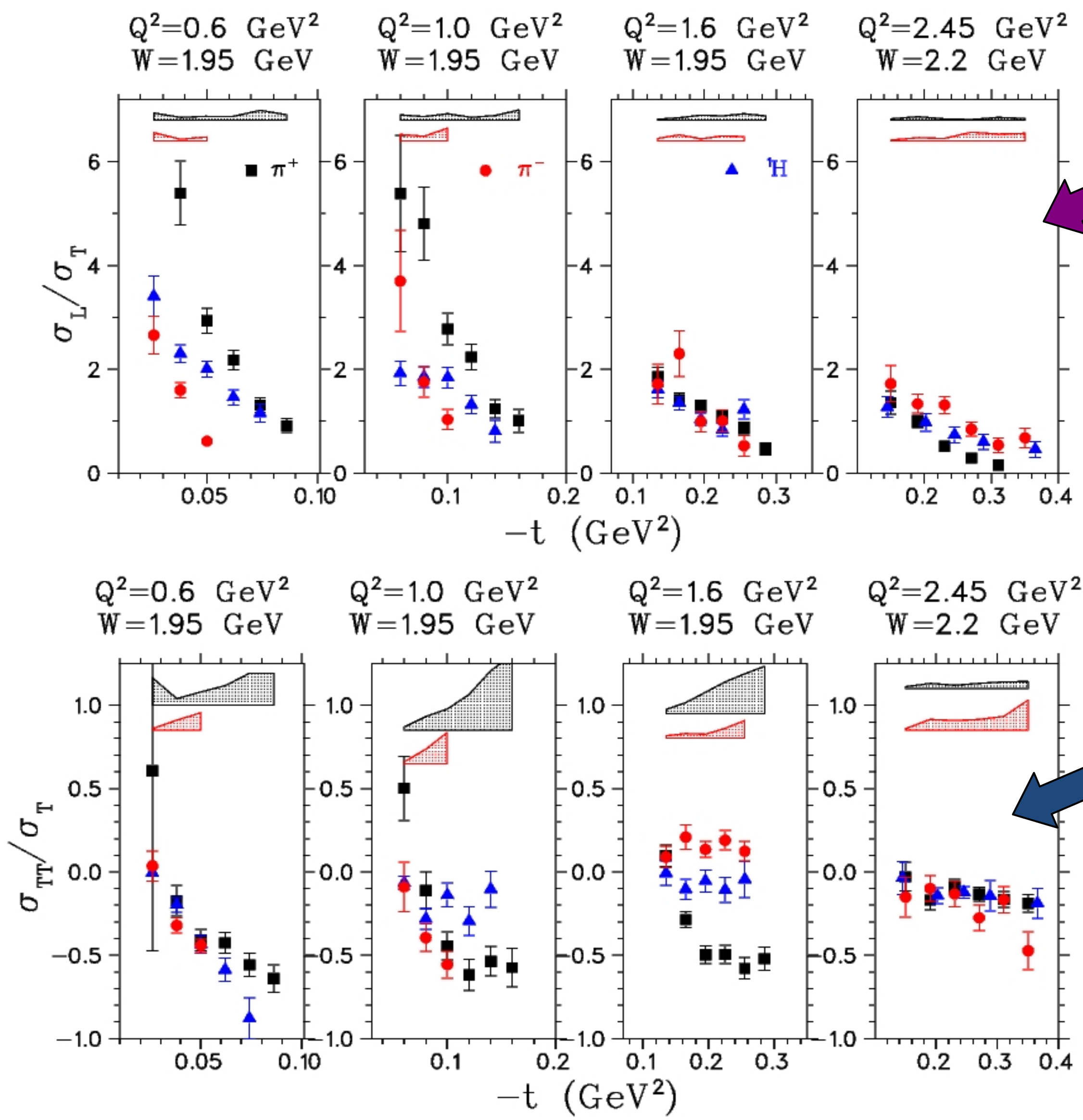

- L/T ratio becomes more favorable for π^- production as Q^2 increases.
- Another prediction of quark-parton mechanism is the suppression of σ_{TT}/σ_T due to *s*-channel helicity conservation.
- Data qualitatively consistent with this, since σ_{TT} decreases more rapidly than σ_T with increasing Q^2.

Error bars indicate statistical and pt-pt systematic uncertainties in quadrature.
Bands indicate MC model dependence systematic uncertainty.

Comparison of Data with Regge-based Models

- Feynman propagator $\left(\frac{1}{t - m_\pi^2}\right)$ replaced by π and ρ Regge propagators.
  - Represents the exchange of a <u>series</u> of particles, compared to a <u>single</u> particle.
- Model parameters fixed from pion photoproduction.
- Free parameters: Λ_π, Λ_ρ (trajectory cutoffs).
- ρ exchange does not significantly influence σ_L at small $-t$.
- Pion form factor is a free parameter in the model, parameterized as:

$$F_\pi = \frac{1}{1 + Q^2/\Lambda_\pi^2}$$

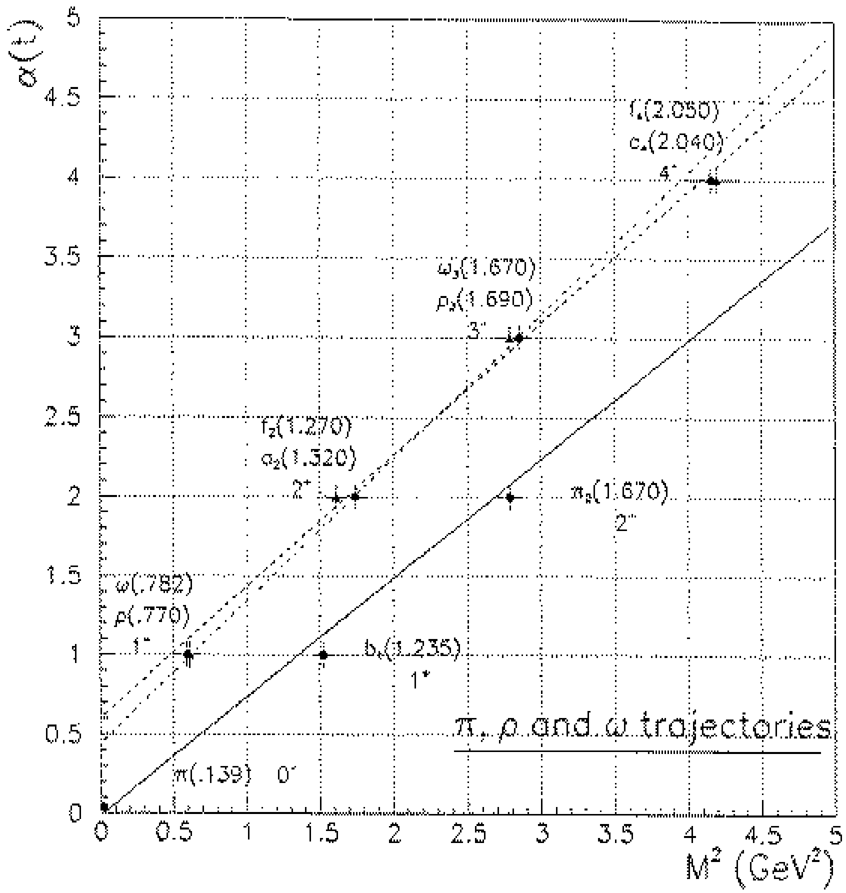

[Vanderhaeghen, Guidal, Laget, PRC **57**(1998)1454]

Model is for nucleon target, no corrections made for ²H effects, such as FSI.

Dr. Garth Huber, Dept. of Physics, Univ. of Regina, Regina, SK S4S0A2, Canada.

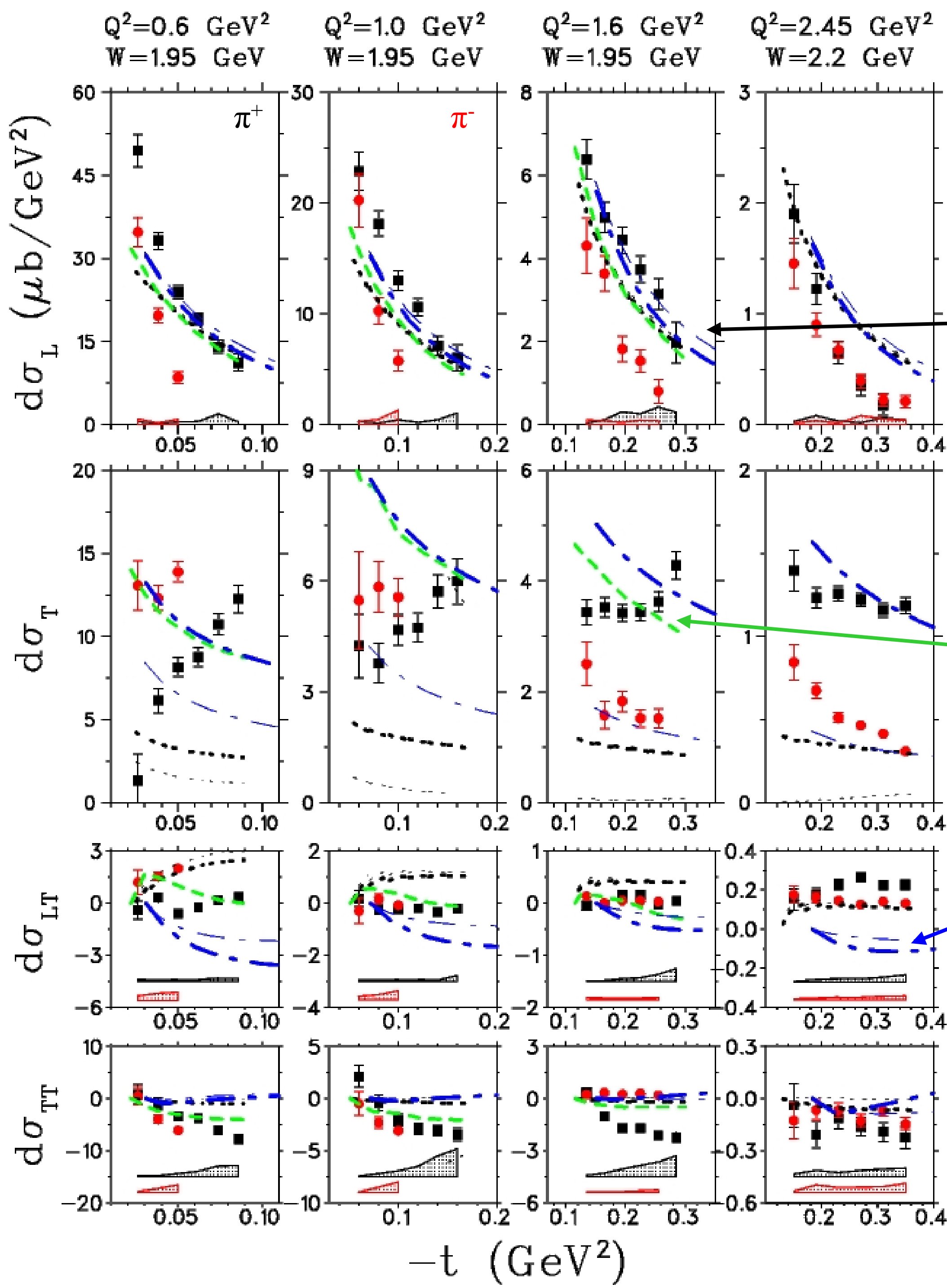

Model $d\sigma_x/dt$

Thick Line: π^+ Calc
Thin Line: π^- Calc

VGL Regge Model:

- Free parameters: Λ_π^2, Λ_ρ^2 (from ^{1}H data).
  [PRC **57**(1998)1454]

KM Regge+DIS Model:

- σ_L from ^{1}H data, DIS process dominates σ_T.
  [PRC **81**(2010)045202]

VR Regge+DIS Model:

- Similar to KM but with improved DIS parameters
  [PRC **89**(2014)025203]

Error bars indicate statistical and pt-pt systematic uncertainties in quadrature.
Bands indicate L,LT,TT MC model dependence systematic uncertainty.

Canada.

Relevance to Pion Form Factor Extraction

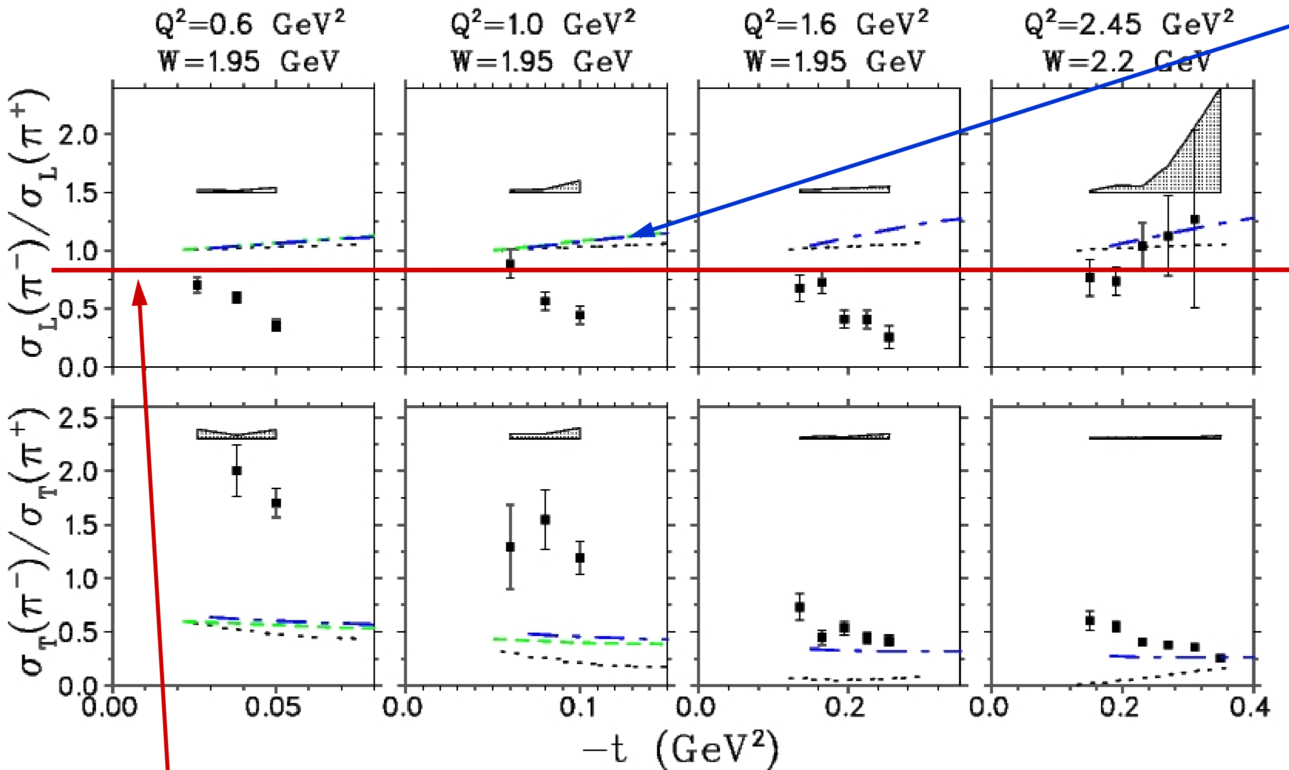

Vrancx-Ryckebusch Regge+DIS Model:

- VGL Regge Model underpredicts σ_T by large factor.
- VR extend Regge model with hard DIS process of virtual photons off nucleons.
- W=1.95 GeV, higher –t data described poorly. [PRC **89**(2014)025203]

R_L=0.8 consistent with $|A_S/A_V|$<6%.

- **Qualitatively in agreement with our Fπ-1 analysis:**
  - We found evidence for small additional contribution to σ_L at W=1.95 GeV not taken into account by the VGL model.
- We found little evidence for this contribution in Fπ-2 analysis at W=2.2 GeV.

Mesons & Baryons

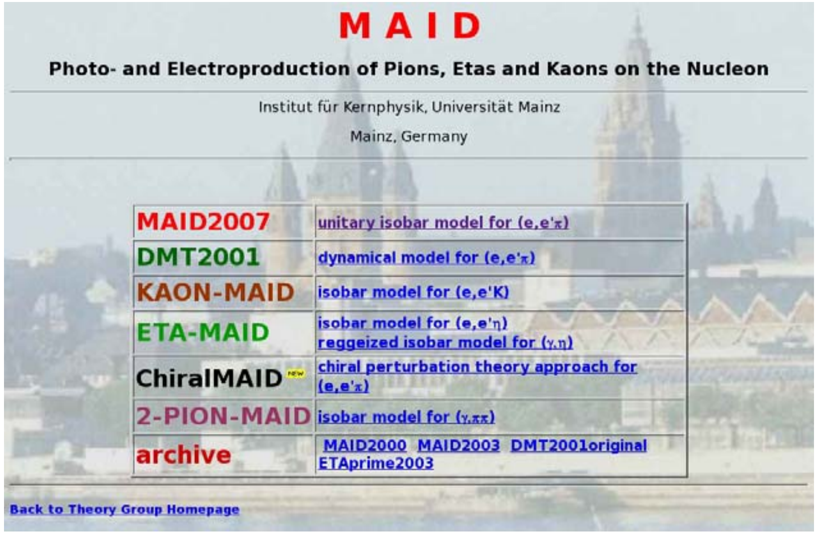

Mainz Unitary Isobar Model

- Phenomenological fit to pion electroproduction data.
- All 13 **** resonances below 2 GeV included.
- **Optimized for W<2 GeV.**

  Drechsel, Kamalov, Tiator, EPJA **34**(2007)69

Hard-Soft Factorization

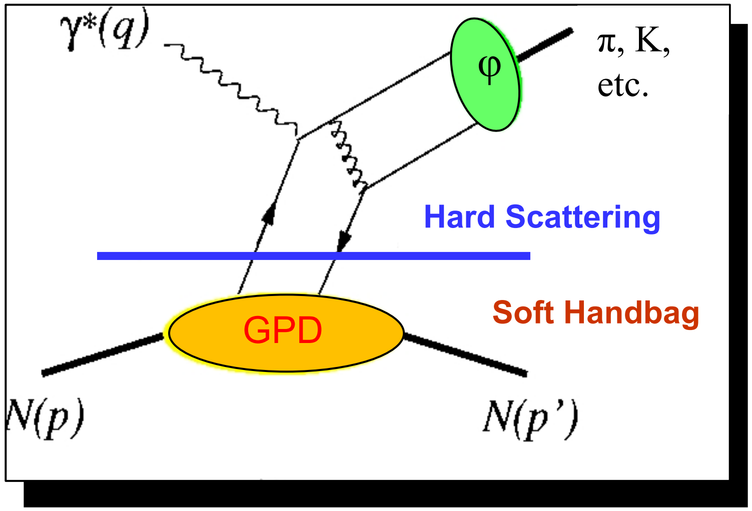

G&K GPD-Based Model

- σ_L based on full $F_\pi(Q^2)$ from ^{1}H data.
- σ_T substantial contributions from twist-3 H_T.
- **Parameters optimized for small skewness (ξ<0.1) and W>4 GeV.**

  Goloskokov & Kroll, EPJA **47**(2011)112

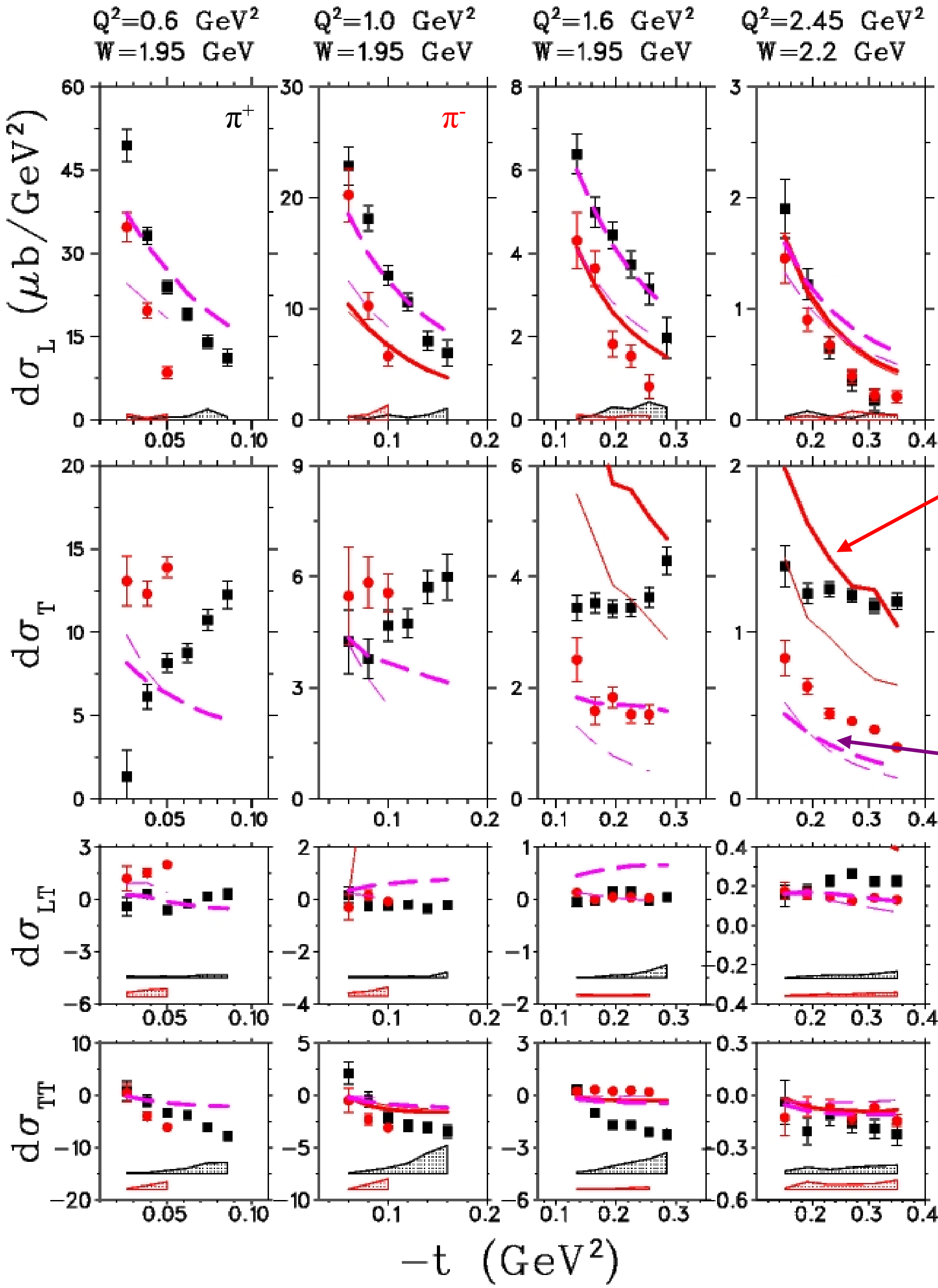

Model $d\sigma_x/dt$

Thick Line: π^+ Calc
Thin Line: π^- Calc

GK GPD-Based Model:

- σ_L based on full $F_\pi(Q^2)$ from ^{1}H data, σ_T substantial contribs from twist-3 H_T.
- **Params optimized for small skewness (ξ<0.1) and W>4 GeV.**

[EPJA **47**(2011)112]

MAID07 Isobar Model:

- Parameters optimized for W<2 GeV.
- Q^2=2.45 GeV^2 results are an extrapolation.

[EPJA **34**(1999)145]

Error bars indicate statistical and pt-pt systematic uncertainties in quadrature.
Bands indicate L,LT,TT MC model dependence systematic uncertainty.

;anada.

Comparison with MAID and GPD models

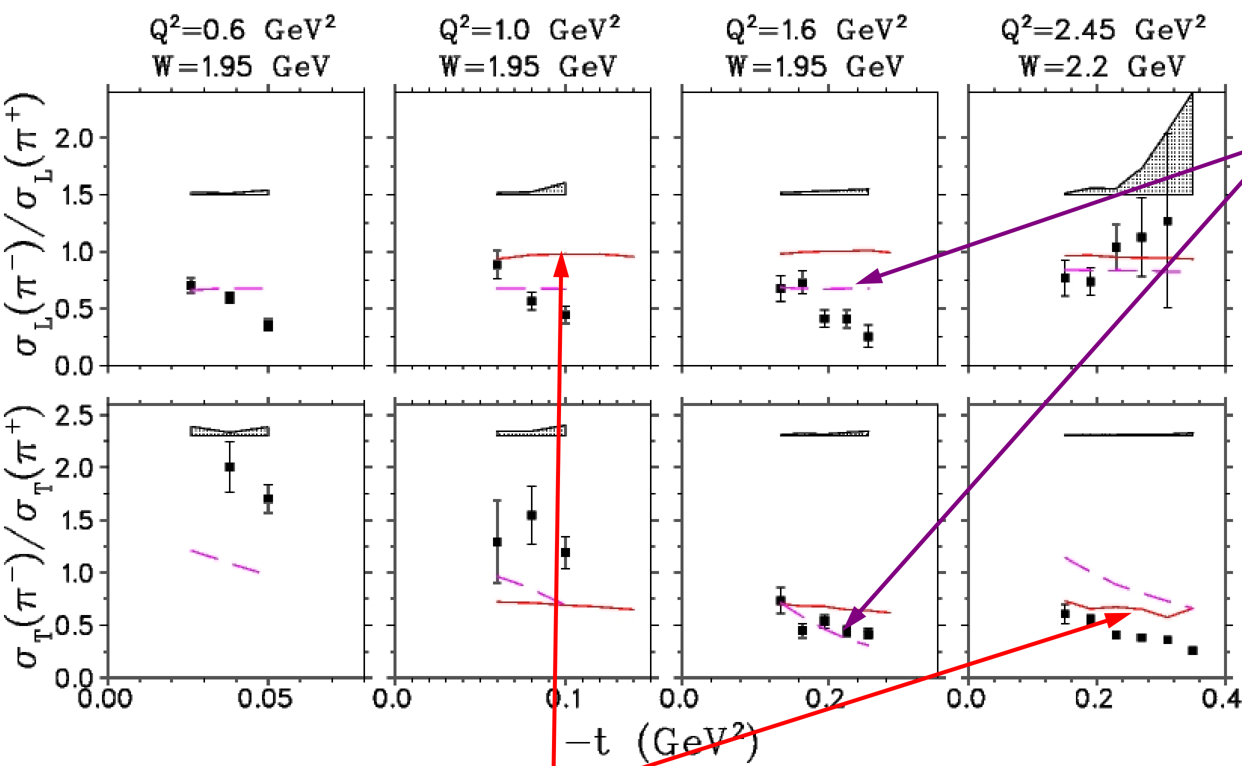

MAID Isobar Model:

- Provides by far the best description of R_L.
- Lends credence that disagreement with pion-pole dominated models is due to small resonant contributions in longitudinal channel.
- Fairly good agreement for R_T at W=1.95 GeV.

GK GPD-Based Model:

- Application to our kinematics requires substantial extrapolation in W, ξ.
  → Please be cautious in the comparison.
- Although model does reasonable job at predicting ratios, agreement of model with our $d\sigma_T/dt$ is not good.
- Model optimized for JLab kinematics should be sensitive to transverse GPD, H_T

12 GeV Upgrade

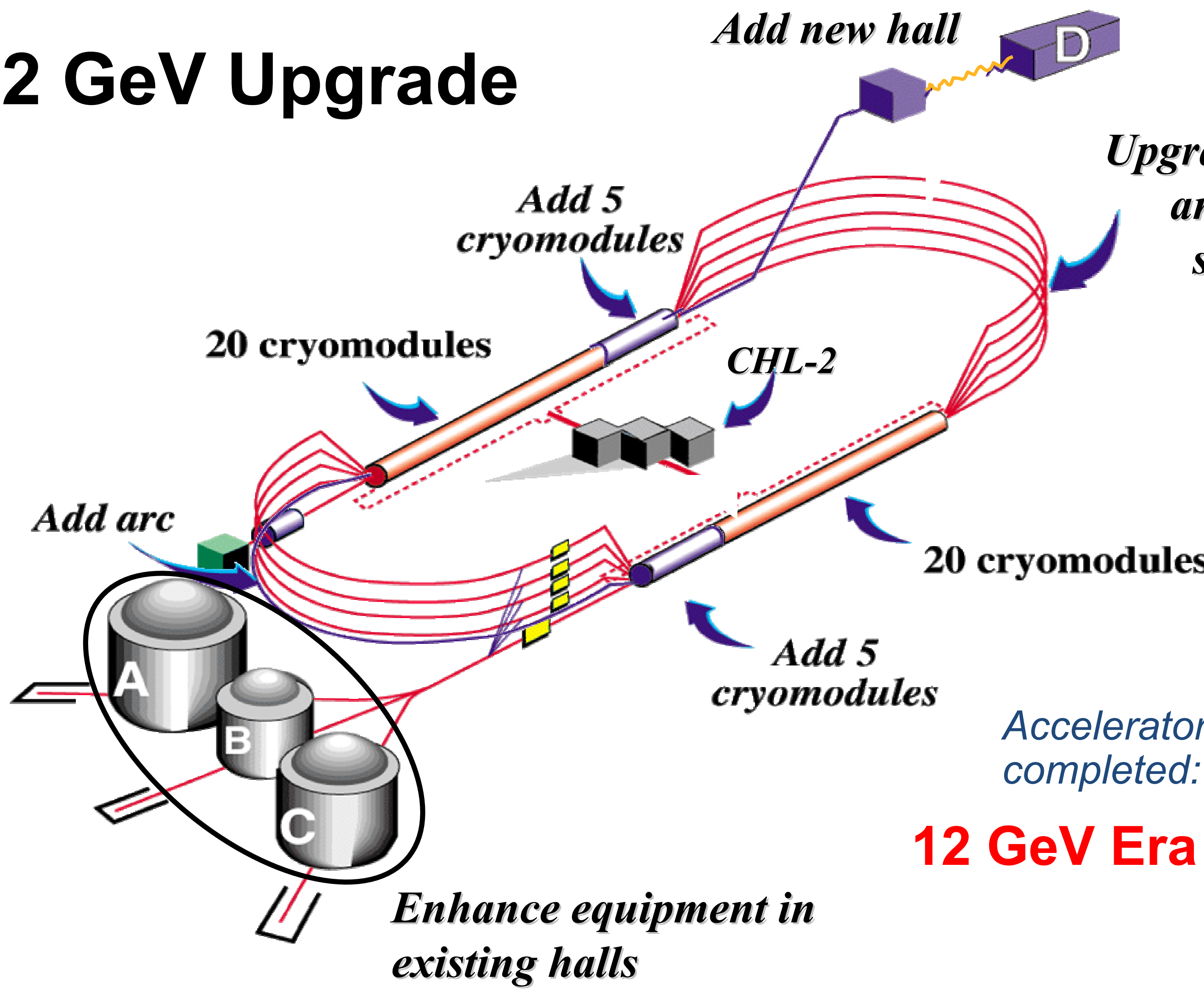

Accelerator upgrade completed: August 2014

12 GeV Era has begun!

Jefferson Lab 12 GeV Era – Hall C Configuration

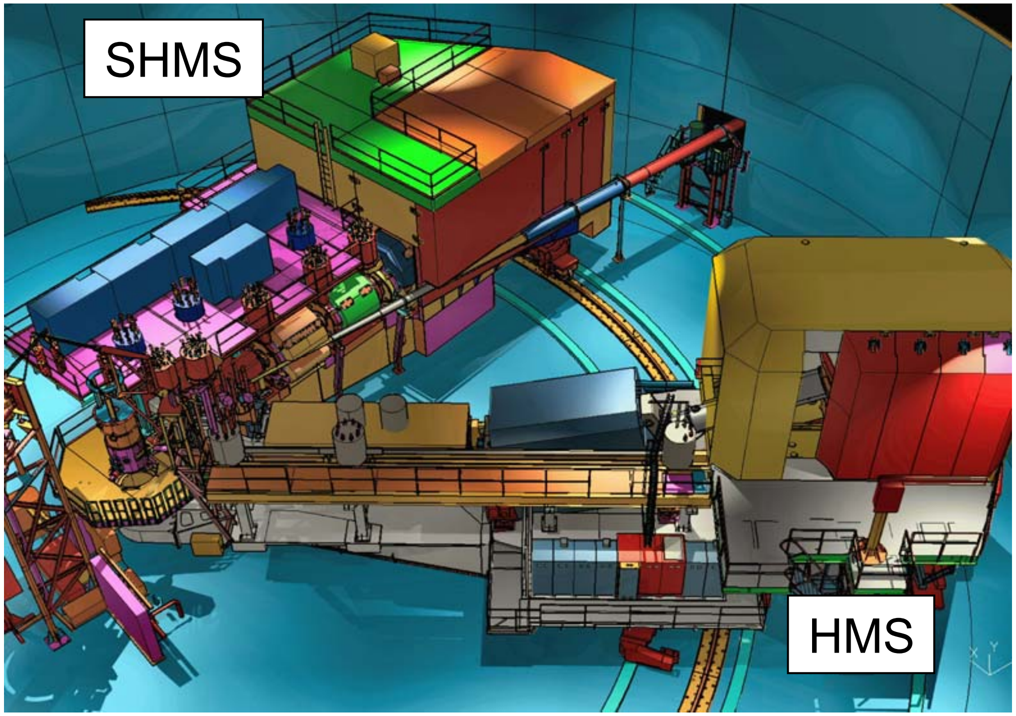

Hall C will provide 2 moderate acceptance, magnetic focusing spectrometers:

High Momentum Spectrometer:
dΩ ~ *6* msr, P_{max} = *7 GeV/c*
Θ = *10.5 to 80 degrees*

Super-HMS :
dΩ ~ *4* msr, P_{max} = *11 GeV/c*
Θ = *5.5 to 40 degrees*

- Both spectrometers provide excellent control of systematic uncertainties
- Kinematic reproducibility, well-understood acceptance

Ideal for:

- precision cross section measurements and response function separations,
    - in single arm or coincidence,
    - at high luminosity (~10^{38}/cm^{2}sec).

Super HMS Overview

Key Features:

– **Horizontal bender magnet**
  - Solution to reasonable acceptance at small angles.

– **QQQ-D**
  - Provides easily calibrated optics and wide acceptance
  - Uses SuperConducting magnets similar to existing HMS where possible

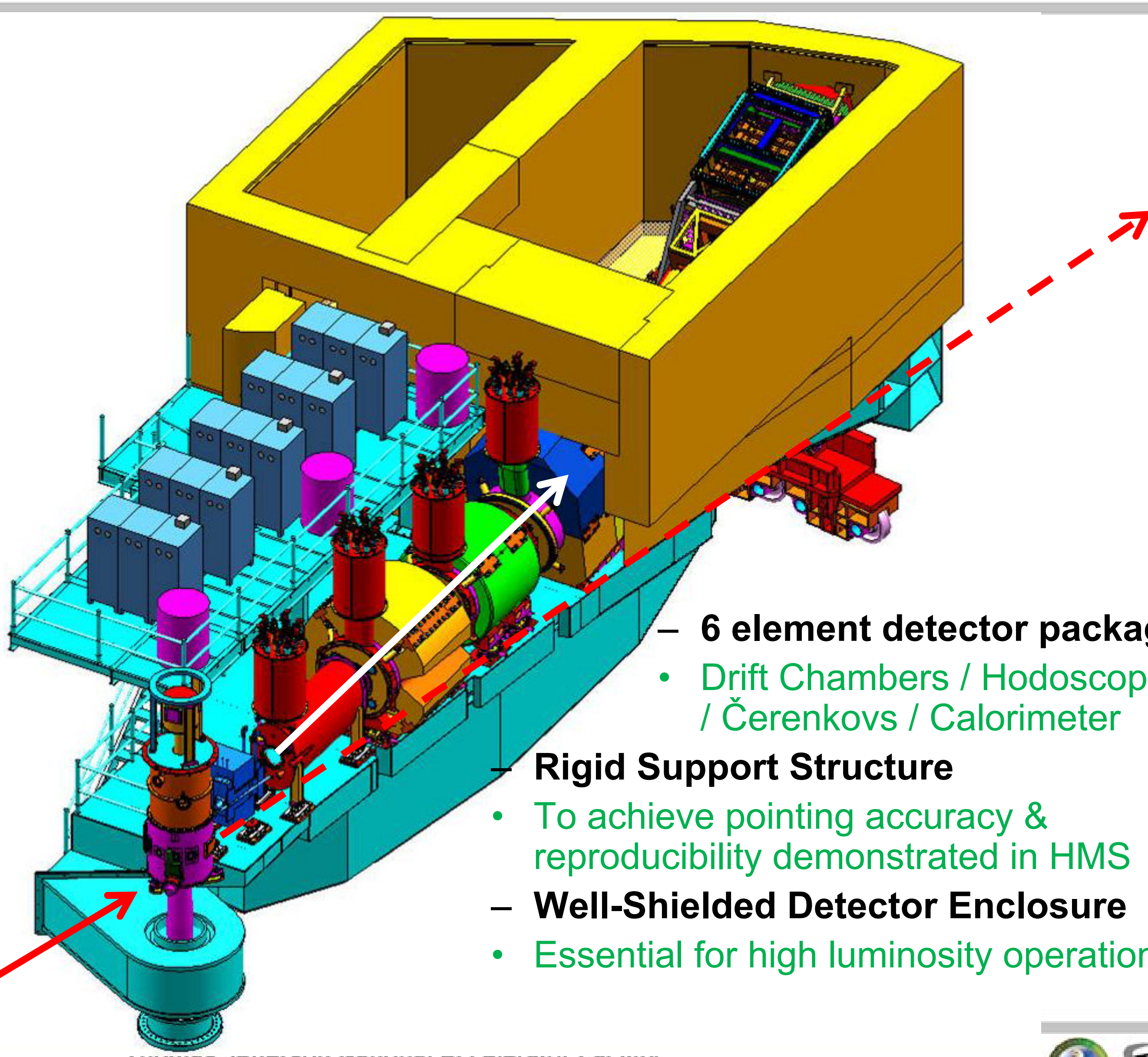

– **6 element detector package**
  - Drift Chambers / Hodoscopes / Čerenkovs / Calorimeter

– **Rigid Support Structure**
  - To achieve pointing accuracy & reproducibility demonstrated in HMS

– **Well-Shielded Detector Enclosure**
  - Essential for high luminosity operation

Engineering for SHMS Small Angle Operation

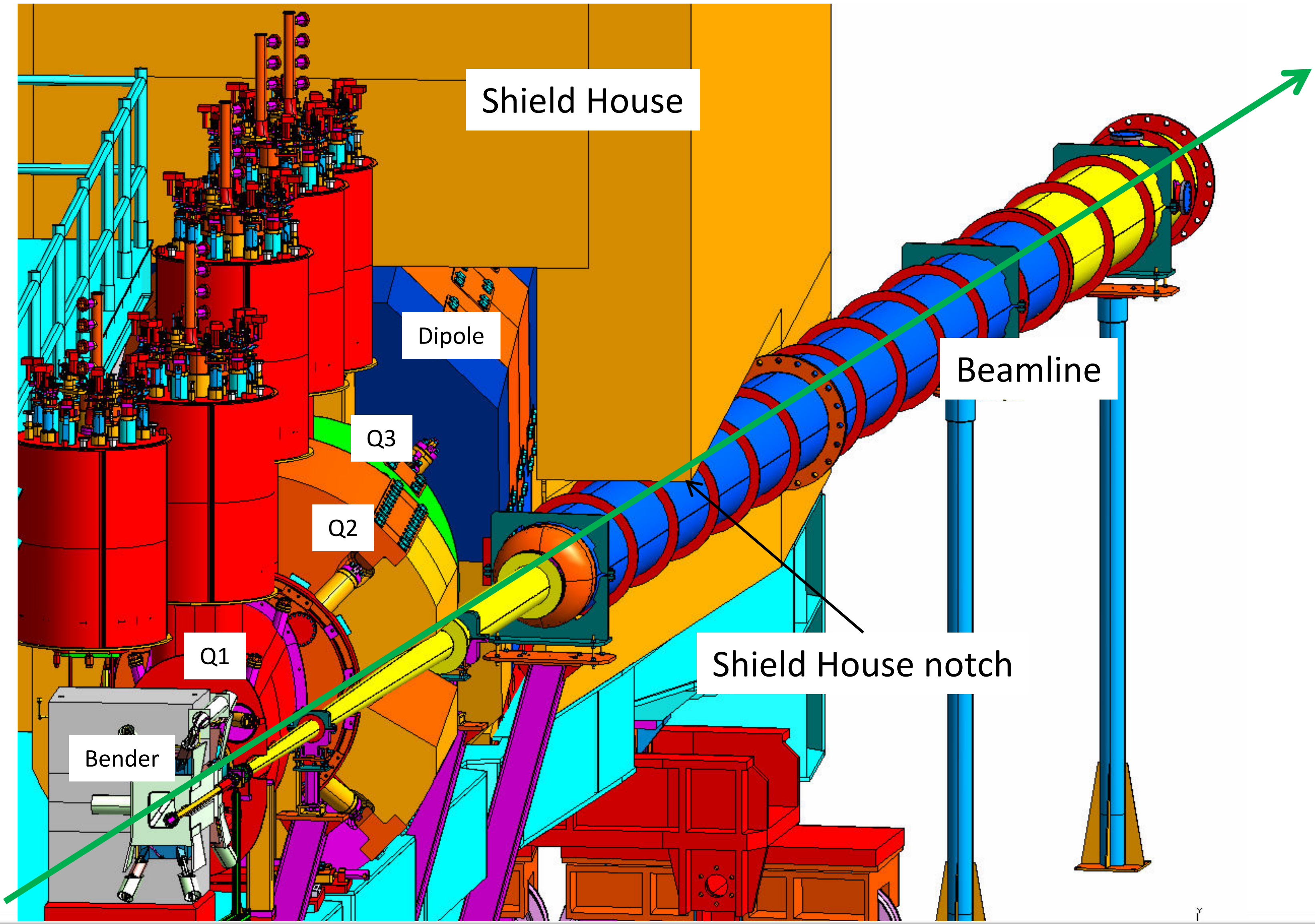

Top View of SHMS-HMS
Minimum Angle Separation for Coincidence Studies

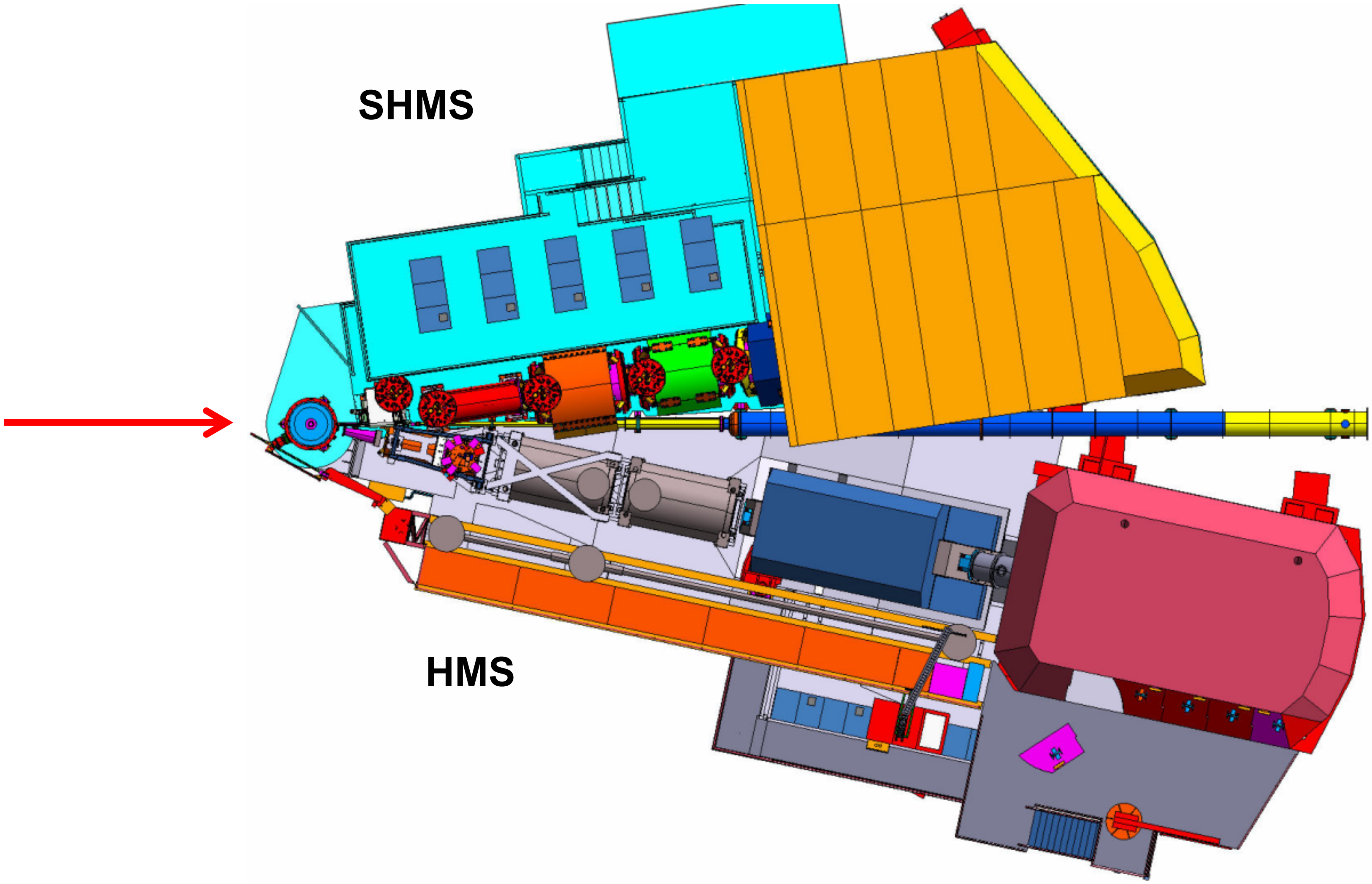

Dismantling the SOS in Early 2013

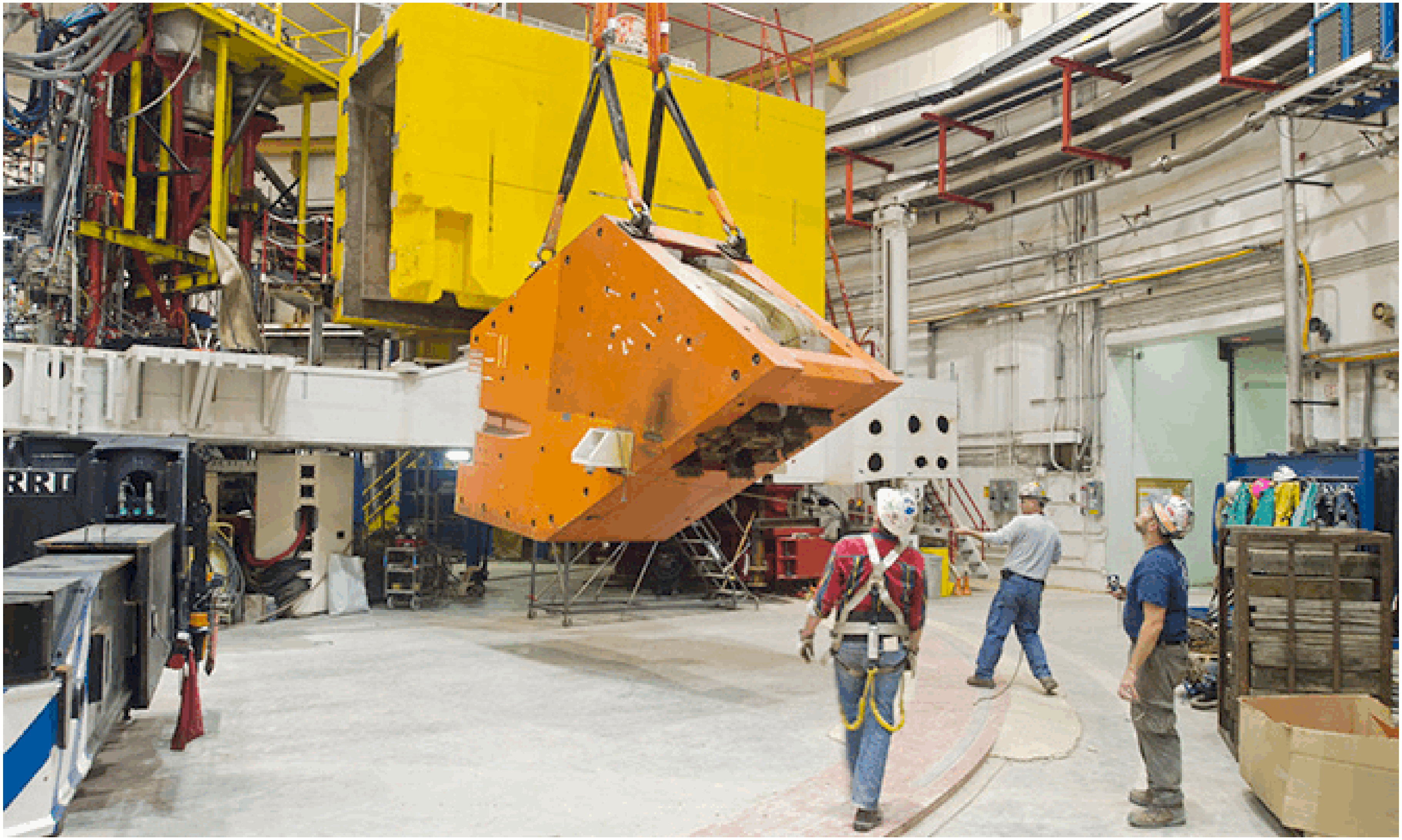

SHMS Support Structure Installation

Platform and Shield House

Magnet power supplies are on the platform.

AC Power Feed is in. Branch circuits, lights, etc., going in now.

Signal/HV Cable pulls done.

Cryogen distribution cans are installed.

June 2, 2014

Superconducting Coil Fabrication

Mold being placed onto Dipole Coil “B” Layers 1&2 in preparation for VPI (May 27, 2014).

Dipole Coil “A” Layer 3 being wrapped and readied for winding layer 4 (May 27, 2014).

JLab Director (Hugh Montgomery), December 5, 2014:
“We expect the first Hall C magnet, Q1, to leave England by ship on December 18. The second magnet, coming from NSCL at Michigan State University, has had its vessel closed in the past week and should be here by spring 2015.
The large dipole coils being fabricated in France have completed winding and by the time you read this article, the Q2 quadrupole coil winding will also be complete. Potting of the dipole coils is in progress.”

SHMS Detector Construction is Complete

Heavy Gas Čerenkov
University of Regina

Horizontal Drift Chambers
Hampton University

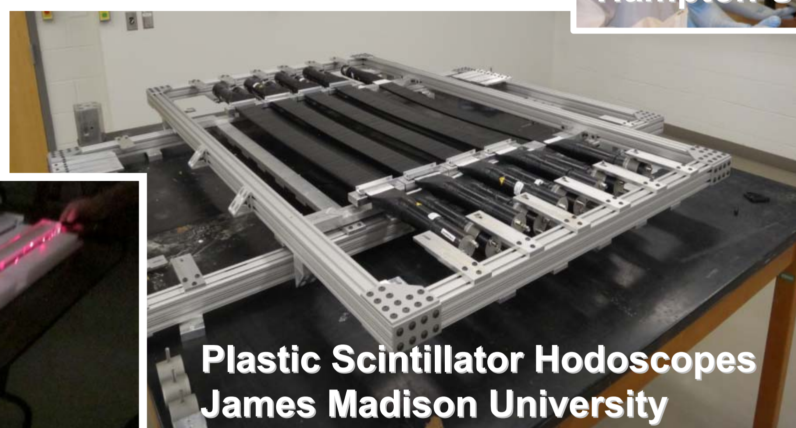

Plastic Scintillator Hodoscopes
James Madison University

Quartz Hodoscope
North Carolina A&T

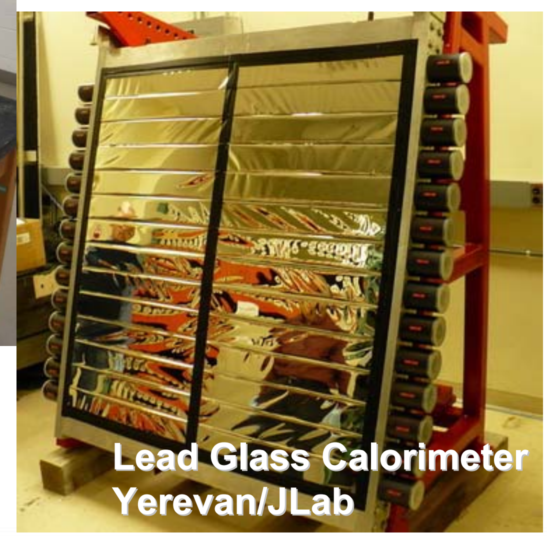

Lead Glass Calorimeter
Yerevan/JLab

Detector Installation on SHMS

Lead Glass Calorimeter Pre-Shower Counter

(November 5, 2014)

Projected Data from Fπ-12 Experiment

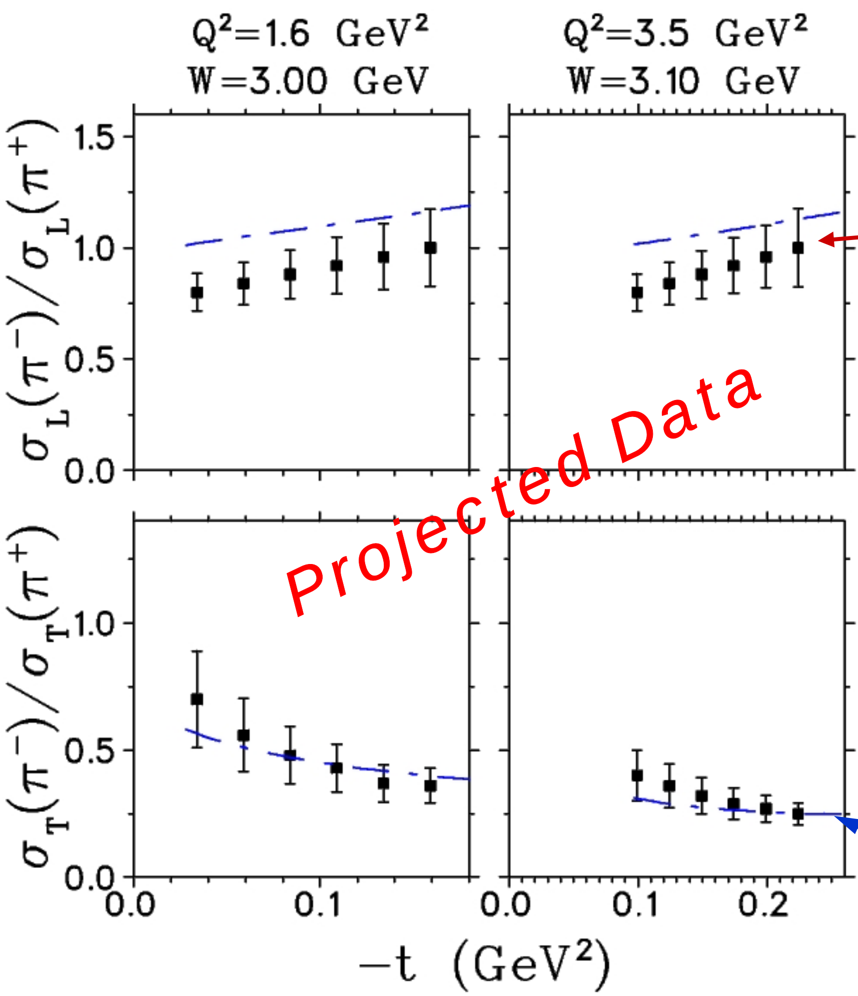

- E12-06-101 approved for 52 PAC-days of beam with SHMS+HMS, A rating, selected by PAC41 as "High Impact".
- ^{2}H data to determine R_L π^-/π^+ ratio to constrain modeling of non-pole backgrounds in σ_L, relevant for extraction of pion form factor
  - 44 hrs (π^+), 174 hrs (π^-).
- If R_T is ~1/4 at higher Q^2 and similar x_B, the hypothesis of a quark knockout mechanism will be strengthened.

Predictions of Vrancx-Ryckebusch Regge+DIS Model
[PRC **89**(2014)025203]

Summary

- **Separated σ_L, σ_T, σ_{LT}, σ_{TT} cross sections for the ^{2}H(e,e'$\pi^\pm$)NN reactions were extracted using the Rosenbluth L/T separation technique.**
  - Fπ-1: W=1.95 GeV: Q^2=0.6, 1.0, 1.6 GeV^2.
  - Fπ-2: W=2.2 GeV: Q^2=2.45 GeV^2.
- **π^-/π^+ ratios for σ_L, σ_T extracted as a function of -t.**
  - R_L≈0.8, trending towards unity at low –t.
    - Indicates the dominance of isovector processes at low –t in the longitudinal response function.
  - The evolution of R_T with –t shows rapid fall, approaching ¼, the square of the ratio of the quark charges involved.
    - Caution needed: MAID model suggests important soft effects.
    - Quark knockout hypothesis would be strengthened if future JLab results at higher Q^2 and similar x_{Bj} also approach ¼.

Jefferson Lab F_π Collaboration

R. Ent, D. Gaskell, M.K. Jones, D. Mack, D. Meekins, J. Roche, G. Smith, W. Vulcan, G. Warren, S.A. Wood
Jefferson Lab, Newport News, VA , USA
C. Butuceanu, E.J. Brash, G.M. Huber, V. Kovaltchouk, G.J. Lolos, S. Vidakovic, C. Xu
University of Regina, Regina, SK, Canada
H.P. Blok, V. Tvaskis
V.U. University, Amsterdam, Netherlands
E. Beise, H. Breuer, C.C. Chang, T. Horn, P. King, J. Liu, P.G. Roos
University of Maryland, College Park, MD, USA
W. Boeglin, P. Markowitz, J. Reinhold
Florida International University, FL, USA
J. Arrington, R. Holt, D. Potterveld, P. Reimer, X. Zheng
Argonne National Laboratory, Argonne, IL, USA
H. Mkrtchyan, V. Tadevosyan
Yerevan Physics Institute, Yerevan, Armenia
S. Jin, W. Kim
Kyungook National University, Taegu, Korea
M.E. Christy, C. Keppel, L.G. Tang
Hampton University, Hampton, VA, USA
J. Volmer
DESY, Hamburg, Germany
A. Matsumura, T. Miyoshi, Y. Okayasu
Tohuku University, Sendai, Japan
B. Barrett, A. Sarty
St. Mary's University, Halifax, NS, Canada
K. Aniol, D. Margaziotis
California State University, Los Angeles, CA, USA
L. Pentchev, C. Perdrisat
College of William and Mary, Williamsburg, VA, USA